We thank the reviewers for the time taken to carefully read the manuscript and the thorough review and comments. We have incorporated most in the edited copy and we feel that these changes have markedly improved the manuscript. We apologize for the somewhat sloppy and sometimes repetitive nature of the manuscript. The paper was created from separate contributions of the co-authors, and it also "suffered" from a late decision to provide this dedicated manuscript on the data. Parts were cut from the draft of the manuscript describing the science. (Wanninkhof, R., Trinanes, J. A., Park, G.-H., Gledhill, D. K., and Olsen, A.: Large Decadal Changes in Air-Sea CO2 Fluxes in the Caribbean Sea,, Journal of Geophysical Research, 10.1029/2019JC015366, 2019.). We have eliminated the repetitive sections.

While all the review comments were very useful, some are outside the scope of ESSD on the presentation of the datasets (see below). For the reviewers comments that pertain to interpretation we largely refer to the 2019 paper, or reference other key papers. We have referred to the Wanninkhof et al. 2019 paper several more times in the edits when appropriate. Specific responses are listed below embedded in the reviewers comments.

"Scope of ESSD: "Earth System Science Data (ESSD) is an international, interdisciplinary journal for the publication of articles on original research data (sets), furthering the reuse of high-quality data of benefit to Earth system sciences. The editors encourage submissions on original data or data collections which are of sufficient quality and have the potential to contribute to these aims."

Interactive comment on "A17-year dataset of surface water fugacity of CO2, along with calculated pH, Aragonite saturation state, and
air-sea CO2 fluxes in the Northern Caribbean Sea"
by Rik Wanninkhof et al.
Anonymous Referee #1
Received and published: 28 February 2020

Formatted: Font: Arial

Formatted: Font: (Default) Arial, 12 pt

A 17-year dataset of surface water fugacity of CO2, along with calculated pH, Aragonite saturation state, and air-sea CO2 fluxes in the Northern Caribbean Sea.

This manuscript presents a straightforward assessment of an impressive dataset taken in the Caribbean Sea aboard two cruise ships outfitted with state-of-the-art CO2 measurement equipment. The CO2 data along with modeled salinity (used to estimate TA), MLD and satellite SST were used in a year by year algorithm to estimate pH and Omega-aragonite. A statistical binning process is used to aggregate these data into 1-degree bins.

This work should be good to be published with minor revisions assuming the comments are addressed.

My most pressing concern centers on using separate fitting algorithms for each year. The authors need to justify this. A quick glance reveals that the differences in the coefficients are quite large year by year. Why wouldn't it make more sense to do this by aggregating seasonal data? When considering the time series data: what would be the effect of the use of annual estimates rather than a single fitting? For example, I wouldn't expect a smooth transition between December and the subsequent January that uses a different algorithm.

We have provided additional justification and show that there are no large offsets from year to year fit in a new figure:

"The MLRs to create the monthly mapped products were produced for each year such that the mapped products could be extended each year in a straightforward fashion. To determine if there were anomalous discontinuities between December and January that could impact the timeseries, the difference in between fCO_{2w} for subsequent months were plotted versus time in Figure 3. No significant discontinuities were observed. Only for Jan 2009, 2010, and 2017 there appear to be a slight difference in the pattern of monthly progressions but such anomalies are observed during other times of year as well. Using an MLR that includes year as one of the coefficients (supplemental material S2 and S3) provides a slightly worse fit. More importantly, using such a fit would necessitate recalculating the mapped products every time a new year is added. "

Also, I do not see good description of how the derived parameters pH and Omega Ar were validated.

Since Omega is calculated, and pH was not measured on the cruise there is no straightforward way to validate these products. We have emphasized that these are products and have added a section and a new Table 2 on estimated uncertainties of the products.

Minor concerns: Line 121. A Licor 6262 was used. While this is a fine instrument, it has not been production since 2005. I'm not worried about the CO2 measurements since they do a good job with standards, but how was the H2O channel calibrated or standardized? How accurate is your pH20?

We have listed that the H2O channel was zeroed, and that water vapor concentration was very low

Section 2.4. What information do the MLD estimates convey? They mention what they could be used for e.g. inventories, but nothing about how they help the estimates. Please include your ideas on this.

We have detailed that this is a gap filling technique

Line 150. The term "bone dry" is not very scientific and should have been hyphenated. Plus, bones are not that dry. See, Timmins, P.A., Wall, J.C. Bone water. Calc. Tis Res. 23, 1–5 (1977). https://doi.org/10.1007/BF02012759.

This is a common expression in the "old" chemistry school. We have eliminated this phrase

Line 150. Mentions "analyses typically had a humidity of 10% or less", but earlier (L. 120) mentioned that the headspace was dried >75%. I think I get the distinction, but it was confusing to me.

This was corrected. It is less than 10 %

Line 267. Mentions that cooler near surface temperatures could lead to lower fCO2 values and that this has a "large impact on the calculated air sea fluxes". Please use a citation or constrain the "Large impact" with some stats. **We added the estimate from the Wanninkhof 2019 paper.**

Formatted: Font: (Default) Arial, 12 pt

Formatted: Font: (Default) Arial, 12 pt

"As shown in Wanninkhof et al. 2019b, a 0.25 ˚C bias in SST leads to a 2 µatm difference in fCO_{2w} and a 25 % change in the air-sea CO_2 flux" and we also provide a brief discussion in the new section on uncertainties, including two new references

Line 273-275. Where does the steady state increase of 2.13 uatm/yr come from? Is this from the ship's atm data, or is it Mauna Loa, carbon tracker or something else. Also, over a 17-year time series, one would expect a changing rate of CO2atm. Is "steady state" referring to the linear increase over that time period? Clarify.

The source of atmospheric data was provided two paragraphs below line 273-275. "For the air-sea CO_2 fluxes, the monthly fCO_{2a} values were derived from the weekly average xCO_{2a} of the stations on Key Biscayne (KEY) and Ragged Point Barbados (RPB) (CarbonTracker Team, 2019; https://www.esrl.noaa.gov/gmd/ccgg/flask.php).

We changed the sentence to" At steady state this atmospheric CO_2 increase would translate to a linear trend of fCO_{2w} of 2.13 µatm yr^{-1} over the time period."

Line 324 For Boron, I though the Lee at al, 2009 algorithm was more commonly used these days. **The verdict is still out. In the SOCCOM project and in Orr et al. 2018 (new reference) the use of Uppström (1974) is recommended. We left this unchanged.**

Line 343. Use a reference or two for the use of Omega as a biological indicator.

We added one specific to corals: Mollica, N. R., Guo, W., Cohen, A. L., Huang, K.-F., Foster, G. L., Donald, H. K., and Solow, A. R.: Ocean acidification affects coral growth by reducing skeletal density, Proceedings of the National Academy of Sciences, 115, 1754, 10.1073/pnas.1712806115, 2018.

Equation 9. If this is right out of CO2sys, I see no reason for an equation.

You would have to dig into the code of CO2Sys and this equation is pretty fundamental, but seldom presented, when discussing saturation states. We left this unchanged.

Figure 1. It's unfortunate that there's little data where the salinity variability is presumably the highest (i.e. in the Southern Caribbean where the large South American Rivers affect the region). What is the effect of this on the gridded data?

As shown in Wanninkhof 2019 (figures 3 and 4) and accompanying text, the salinity anomalies show up in the SE and NW part of the region. However, these variabilities in salinity have a small effect on the total area.

Acknowledgments: should mention the cruise line that made this possible.

Yes, thanks for pointing this out. We had RCCL listed in the team list but we have added the following in the acknowledgement : "This work would not have been possible without support from Royal Caribbean Cruise Lines who have provided access to their ships and significant financial, personnel, and infrastructure resources for the measurement campaign coordinated through the Rosenstiel School of Marine and Atmospheric Sciences of the University of Miami."

Interactive comment on "A17-year dataset of surface water fugacity of CO2, along with calculated pH, Aragonite saturation state, and
air-sea CO2 fluxes in the Northern Caribbean Sea"
by Rik Wanninkhof et al.
Anonymous Referee #2
Received and published: 1 March 2020

The manuscript presents a dataset of surface ocean fCO2, and auxiliary variables, measured in the Caribbean from 2002-2018. In addition, a data product consisting of gridded and gap-filled maps of fCO2, pH, aragonite saturation state, and air-sea CO2 fluxes is produced and presented. Both the observational dataset and the data products are of undoubtedly high quality and will very likely be very useful to the global ocean carbonate chemistry community. The manuscript is nicely presented and illustrated, and overall well-written though at times

highly repetitive. This work is highly relevant for publication in ESSD and can be published after minor revisions (detailed below)

Major comments:

Why use annual multilinear regressions? I understand from the appendix that using delta_fCO2 did not improve the results, but I'd like to also see what difference it would make to use one multilinear regression where atmospheric xCO2 (or fCO2) is included as a predictor variable. Have you analyzed whether the use of annual multilinear regressions create discontinuities between December and January? Please add a figure showing that this is negligible.

This was noted by reviewer 1 as well. We have provided additional justification and show that there are no large offsets between year to year fits:

"The MLRs to create the monthly mapped products were produced for each year such that the mapped products could be extended each year in a straightforward fashion. To determine if there were anomalous discontinuities between December and January that could impact the timeseries, the difference in between fCO_{2w} for subsequent months were plotted versus time in Figure 3. No significant discontinuities were observed. Only for Jan 2009, 2010, and 2017 there appear to be a slight difference in the pattern of monthly progressions but such anomalies are observed during other times of year as well. Using an MLR that includes year as one of the coefficients (supplemental material) provides a worse fit. More importantly, using such a fit would necessitate recalculating the mapped products every time a new year is added. "

I find the entire manuscript to poorly structured which results in a lot of repetition. I suggest to restructure in order to create a nicer flow of information and thus increase readability. Some suggestions, in no particular order: - The information on lines 94- 104 would be better suited in

section 1.3 (instrumentation) - Information in section 1.3 (instrumentation) and sections 2.1 and 2.2 should be combined and the text screened for repetitive information (e.g., the frequency of calibration is mentioned on line 114 and again on line 122)

While we have retained the structure, we have rearranged the text and eliminated repetition as shown in the uploaded version of the manuscript using MS-Word track changes and it is more readable now.

- I'm not sure of the value of section 1.3.3 unless these data are used in the presented dataset or data products (which is unclear)

This is to indicate that this UWpCO2 system is part of a larger effort. This also points readers to a possible opportunity to utilize these observations in conjunction with UWpCO2 data and data products presented

- Section 2 could be a subsection under section 1 - Much of the information on lines 65-74 would be more appropriate in the methods (much of it is also repeated in the different methods sections) - The information on lines 270-294 would be better suited in section 3.5 - In section 4.1 you give much information which is suitable, and partly repeated, in section 5

We've made significant edits along the lines suggested but retained the overall structure. E.g. section 1. Is about instrumentation, section 2 is about data from the instrumentation. For readers who are more interested in the data it avoids needing to closely read the detail of the instruments themselves.

Minor comments:

Line 64: I'd prefer the term "raw data processing" over "data reduction". While the former is commonly used in the community, it is not intuitive to those outside what it actually involves

We are confused by this comment as it suggests that the recommended change to "raw data processing" is not intuitive. We agree with that as "raw data" is a bit ambiguous and we kept nomenclature as is.

In the introduction it is stated that the Explorer of the Seas changed her home port to Bayonne, NJ in 2008 while in section 1 it is stated that the new home port is Cape Liberty Cruise Port. I realize these may be in the same place but it is nevertheless confusing.

Thanks for pointing this out it was changed

Please revise Line 171: Explain what flag questionable is (presumably WOCE 3)

Done

Line 242: I do not understand the method. Please explain. Line 340-341: While this is correct I find it helpful to instead state that when omega_Ar<1 dissolution is thermodynamically favored, and vice versa when omega_Ar>1. In living organisms both dissolution and precipitation of calcium carbonate is biologically mediated, and shells have been shown to survive well in water with omega_Ar 0.9.

Based on this reviewers comments, and that of reviewer one, we have changed the text to "When Ω_{Ar} is less than 1 dissolution is thermodynamically favored and when Ω_{Ar} is greater than 1 aragonite would have a tendency to precipitate."

In section 4 you should define the difference between a dataset and data products. My experience is that surprisingly many do not know the difference. It is unclear whether you consider the gridded data part of the dataset or a data product.

We've adopted following nomenclature [following Wanninkhof et al. 2019]and checked for consistency throughout the paper:

Data : individual data points (observations)

Gridded data: binned and averaged data (in this case monthly on a 1 by 1 grid)

Gridded data product: a derived (calculated or interpolated) (in this case monthly on a 1 by 1 grid)

Mapped data (product): interpolated using the MLRs

Interactive comment on “A17-year dataset of surface water fugacity of CO2, along with calculated pH, Aragonite saturation state, and
air-sea CO2 fluxes in the Northern Caribbean Sea”
by Rik Wanninkhof et al.
Anonymous Referee #3
Received and published: 2 March 2020

The manuscript describes a 17 year dataset for surface water marine carbonate data collected using multiple ships within the Caribbean and a substantial set of derived data.
The manuscript appears to have been a little rushed. There are instances of unclear statements, inconsistent naming, repetition, use of non-SI units, formatting errors and some structural issues. I have listed all comments referring to these issues under the section ‘Minor comments’ (See below).
These issues were also brought up by the other reviewers and we have addressed these and/or provided detail about changes (or why not) below. The issue of non-SI units is noted but we use the community accepted terms of expressing fCO2 in µatm and pressure in millibar. This is done almost exclusively in ocean carbon cycle research.

I would suggest that the manuscript is re-considered after revision and my reasoning is explained below within the Major comments.
Major comments: 1. The uncertainty information within the manuscript is inconsistent and/or incomplete. Some information is given for the fCO2 data but nothing is given for the temperature or salinity. No uncertainty information or statements are given for the derived datasets eg pH or aragonite saturation state or gas fluxes. This limited information will limit the use of these data, or could result in users making incorrect assumptions about the uncertainties. It would be good if the authors could follow a standard framework or phrasing for presenting the uncertainty information e.g. BIPM 2008 framework and identifying if

uncertainties are Type A or Type B and also identify which components of the uncertainty budget have been considered and which have been ignored. Its clear that the derived datasets are unlikely to be considered to be 'truth' measurements, so the authors need to write some text to explain this, so that users of the dataset don't make the mistake of assuming that these data are truth. It may make sense, and/or make it easier for the reader, if all of the uncertainty information was grouped together into a common location (eg one table?) which can then be referred to within the different sections of the manuscript.

BIPM, 2008 - Guide to the expression of uncertainty https://www.bipm.org/utils/common/documents/jcgm/JCGM_100_2008_E.pdf

Formatted: Font: (Default) Arial, 12 pt

Formatted: Font: (Default) Arial, 12 pt

We appreciate the recognition of the reviewer of the importance of characterizing uncertainty that is lacking in many manuscripts covering the environmental sciences, including this one. The guide is also appreciated and read (during this time of shelter at home). We have added a section of uncertainty estimates on the data products following the nomenclature and approach outlined in Orr et al. 2018. The uncertainties in the observations using the instrumentation described and the calculated fCO_{2w} has been described in Pierrot et al, 2006. While full characterization of the uncertainty in the data products is challenging we feel that this new section is an important addition.

lines 266 to 268. The text states that the cooler temperatures near the surface could lead to lower fCO2 which can have large impact on the calculated air-sea gas fluxes. But the gas fluxes have been calculated using a version of the bulk flux calculation (equation 4) which ignores all vertical temperature gradients. However the dataset includes OISST data which could be used to perform a more accurate gas flux calculation (e.g. re-calculate pCO2 to a common depth, then perform a more accurate calculation). The authors could either provide the results using a more accurate gas flux calculation or highlight this issue to the user/reader and then refer to them to an example analysis that shows the impact of a lower accuracy gas flux calculation and

he estimate the increased uncertainty within their derived dataset that results from this lower accuracy calculation. To help, see figures 3 and figure 4 of Holding et al., (2019) for an analysis of the impact along single cruise tracks, or panel 1 of Shutler et al., (2019) for the impact over larger spatial and temporal areas.

Holding et al., (2019) https://www.ocean-sci.net/15/1707/2019/ Shutler et al. (2019) https://esajournals.onlinelibrary.wiley.com/doi/pdf/10.1002/fee.2129

Formatted: Font: (Default) Arial, 12 pt

Formatted: Font: (Default) Arial, 12 pt

This is a description of the mapped product using the conventional bulk flux parameterization as described. This is the same approach as in most climatologies. We are aware of the developments and claims of superior ways of determining the fluxes by normalizing to a common depth and using skin temperatures. We have added a short description in the uncertainty section and referenced two key papers addressing the cool skin effect controversy. This is mentioned in the Wanninkhof 2019 paper as well .

its not clear why the multi-linear regressions are performed and/or why anyone would want this output. These results and methods should introduced giving an explanation as to why they are useful. I'm not sure that this part of the dataset is needed though.

We have clarified that this is the means of mapping for gap filling.

As mentioned:" The gridded observations (1˚ by 1˚ by mo) represent about 10 % of the area of investigation from 15-28 ˚N and 88-62 ˚W over the period of investigation"

so there has to be a means to fill in the missing cells. As described in Wanninkhof et al. 2019, and here the variation in each grid cell provided: "The standard deviation (stdev) of the fCO_{2w} in each cell is determined and then the average of the stdev for the 9924 cells with observations is taken. The average stdev is 3.4 ± 2.6 µatm (n=9224) indicating the small variability in each cell. The same procedure is followed for SST and SSS yielding values of 0.22± 0.19 ˚C for SST; and 0.10± 0.10 for SSS. These are relatively small deviations compared to the monthly spatial range of ≈ 20 µatm for

fCO_{2w}; ≈1 ˚C for SST; ≈ 1 in SSS. The amplitude of the seasonal cycle of ≈ 40 µatm for fCO_{2w} and ≈4 ˚C for SST is significantly greater than the average stdev as well

2. The binning method does not account for the paired nature of the pCO2 and SST datasets (as each parameter is binned individually). Surely the binning will have skewed this relationship and so the paired nature will no longer exist. This issue may be especially true if some bins contain data from multiple cruises (which fig 1 suggests will occur). Can the authors highlight this issue and discuss the implications so that users of the dataset are aware of this problem?

We are not completely clear what the reviewer is getting at. As listed the stdev of the binned and averaged data is quite small and the analysis does not rely on the paired nature of pCO2 and SST. "The standard deviation (stdev) of the fCO_{2w} in each cell is determined and then the average of the stdev for the 9924 cells with observations is taken. The average stdev is 3.4 ± 2.6 µatm (n=9224) indicating the small variability in each cell. The same procedure is followed for SST and SSS yielding values of 0.22± 0.19 ˚C for SST; and 0.10± 0.10 for SSS. These are relatively small deviations compared to the monthly spatial range of ≈ 20 µatm for fCO_{2w}; ≈1 ˚C for SST; ≈ 1 in SSS. The amplitude of the seasonal cycle of ≈ 40 µatm for fCO_{2w} and ≈4 ˚C for SST is significantly greater than the average stdev as well"

Minor comments: 1. line 30, suggest 'The data and products could be used for de- termination of ....' as surely the paper is providing data for others to use (rather than presenting their use of these data).

This merely provides examples of possible use.

2. the use of the word 'average' throughout the manuscript is ambiguous. do the authors mean a statistical mean, mode or median? (all are averages). suggest that all instances of the word 'average' are replaced with the appropriate statistical name.

As listed in section 4.2.1 of the BIPM, 2008 - Guide to the expression of uncertainty. "arithmic mean or average". When we refer to average are referring to the arithmic mean. I am not familiar with calling mode or median an average

3. there are instances of 'month' and 'mo'. the latter I think also means 'month'. I'd suggest that the authors use one throughout, rather than swapping between both. 4.

Thanks. We only use "mo" in units and when describing the grid cell and this is mentioned the first time it is used : "For the regionally mapped products on a 1-degree grid and monthly timescale (1˚ by 1˚ by mo)". The grid size (1˚ by 1˚ by mo) is listed a lot in part based on a reviewers request to the JGR Wanninkhof et al. 2019 paper. For clarity we have placed brackets around each occurrence of (1˚ by 1˚ by mo)".

line 99, space needed between 100 and units (m).

Thanks, done

3. line 101, no dash needed in '5-m'. similarly three further instances on line 109 and more instances of this on line 191.
Thanks, corrected I am always confused when a dash is needed

4. line 126, the value of 2uatm is twice the size of the value on line 120. are these the same values ie +-1uatm? how has this value of 2uatm been estimated?
This is provided in the reference that is now added , "estimated at better than 2 µatm (Pierrot et al., 2009)," The intercomparison showing 1 uatm agreement used common standards, pressure and temperature measurements. The 2 uatm incorporates uncertainties in Teq and P as described in the provided reference.

5. line 115, I'd suggest '...measurements for the ships with ir intakes and analysers.' 8. line 124. can you provide the range in values used for the standards?
Added in the description of the standards " The four calibration gases supplied by the global monitoring division of the environmental science research laboratory of NOAA (GMD/ ESRL/NOAA) are traceable to the WMO CO_2 mole fraction scale. The CO_2 concentrations of the standards span the range of surface water values encountered along the ship tracks (≈ 280- 480 ppm),.

6. section 1.3.2 the precision, accuracy and sensitivity of these instruments are missing.
We have now stated that these can be found in Pierrot et al (2009). However, we do not include sensitivity

7. line 150, use of non scientific phrasing, what is 'bone dry'?
This has been replaced . As noted, "bone dry" used to be the common terminology: "bone-dry=completely dry"

8. line 158, can you define what you mean by infrequently? eg. %age of time.
Change to "Infrequently (<1 % of the time)"

9. line 160. processing routines are mentioned but no detail is given. could an overview of these processing routines be provided in the appendices? this information would appear fairly important should anyone want to use these data and/or try and follow the same methods for a similar effort somewhere else in the world.
The processing routines are described in Pierrot et al. (2006) and as listed MATLAB routines are available from Pierrot on request.

10. line 266, I'd suggest 'While both differences include zero within their uncertainty..'
Done

11. Suggest that section 3.4 (binning procedure) comes before the sections on the calculations (as surely the binning is done first, then the calculations are performed).
We've rearranged the sections and clarified procedures. The fCO_2 and pCO_2 was calculated and then the results were binned. For the fluxes we used the binned product. So placing it before the fluxes would make sense but it does not flow as well. Added a reference to the following section "a bulk formulation is applied to the data from the gridded mapped product (see 3.4):"

12. line 303, I think that CCMP data are available for 2018 eg http://data.remss.com/ccmp/v02.0/
Yes but this was not available when the calculations were performed. These will be annual updates and when the 2019 data is included the winds will be updated

Formatted: Font: (Default) Arial, 12 pt
Formatted: Font: (Default) Arial, 12 pt

13. line 327, see 'were compared for 201'. what is 201?
Corrected to 2017

14. line 336, 'insignificant' is a bit subjective and application specific. can you put this into context?
We have changed this and included it in the discussion of uncertainty

"This MLR was then applied to the independent variables for each grid box to determine pHT(MLR). This was compared to the approach used here of calculating the pH using the mapped fCO2wMLR and TA-SSS relationships on (1˚ x 1˚ x mo) grids, called pHT(fCO2w,TA). The two approaches provided similar results with pHT(fCO2w,TA) - pHT(MLR) = -0.0001 ± 0.005 for 2017. The small difference showed a pattern with SST (Fig. 6) but not with the other independent variables. The differences using either pHT(fCO2w,TA) or pHT,MLR are an order of magnitude smaller than the combined standard uncertainties such that the approach of using mapped fCO2w and TA to determine pHT(MLR) yielded precise and consistent gridded pHT."

15. table 3, space needed between 12 and (December).
done

16. table 3, 4, and 5 all contain non-SI unit notation in pH row (mol/kg-SW)
unclear pH is unitless as indicated

17. line 407, the 'stdev' has previously been used, but not defined.
Defined in section 3.4: " The standard deviation (stdev) of"

18. the content in section 4.5 is a bit jumbled. The method for the annual and monthly values needs to be more clearly and sequentially explained. Eg surely the values are first weighted by area and then summed (rather than summed and the mean value area weighted?).
Thanks. This section has been rewritten

19. line 411 to 414. Can you clarify this paragraph? I'm afraid that I don't really understand this paragraph or the reasoning and why are the data treated differently?
Thanks. This section has been rewritten

20. line 409, the dash between terra and grams is not needed.
Done

21. section 5 contains repetition (with section 4.1).
The data availability section is a requirement for ESSD and it also must appear in the main text.

22. line 445, I'd suggest '..instrumental in maintaining the science operations.'
Done

23. line 667, month/year notation is different from the main paper.
We've made it consistent

24. line 676, how is this 'overall uncertainty' determined?
Changed to combined Standard uncertainty in the $fCO_{2w,MLR}$ as per Orr et al, 2018

25. line 677, mixing of 'errors' and 'uncertainties' naming. I think that they are all uncertainties (error implies that you know a truth value). What is the 'error' column in table 1? and it appears to be called RMSE in table A1 and A2.
We have defined the abbreviations in the footnote. Error is standard error

26. line 683, Lat and Lon not defined.
Corrected and changed LAT and LON in tables to Lat and Lon

27. line 684, RMS not defined.
Corrected

A 17-year dataset of surface water fugacity of CO_2, along with calculated pH, aragonite saturation state, and air-sea CO_2 fluxes in the Northern Caribbean Sea

Rik Wanninkhof[1], Denis Pierrot[1,2], Kevin Sullivan[1,2], Leticia Barbero[1,2], and Joaquin Triñanes[1,2,3]

[1]Atlantic Oceanographic and Meteorological Laboratory (AOML), NOAA, 4301 Rickenbacker Causeway, Miami, FL 33149 USA

[2]Cooperative Institute for Marine and Atmospheric Studies, Rosenstiel School of Marine and Atmospheric Science, University of Miami, 4600 Rickenbacker Causeway, Miami, FL 33149 USA

[3]Laboratory of Systems, Technological Research Institute, Universidad de Santiago de Compostela, Campus Universitario Sur, Santiago de Compostela, 15782, Spain

Correspondence to: Rik Wanninkhof (rik.wanninkhof@noaa.gov)

Deleted:

Deleted: Aragonite

Abstract. A high-quality dataset of surface water partial pressure/fugacity of CO_2 (pCO_{2w}/fCO_{2w})[1], comprised of over a million observations, and derived products are presented for the Northern Sea covering the timespan from 2002 through 2018. Prior to installation of automated pCO_2 systems on cruise ships of the Royal Caribbean Cruise Lines and subsidiaries, very limited surface water carbon data were available in this region. With this observational program, the Northern Caribbean Sea has now become one of the best sampled regions for pCO_2 of the world's ocean. The dataset, and derived quantities are binned and averaged on a 1-degree monthly grid and available at http://accession.nodc.noaa.gov/0207749, DOI:10.25921/2swk-9w56 (Wanninkhof et al., 2019a). The derived quantities include total alkalinity (TA), acidity (pH), Aragonite saturation state (Ω_{Ar}) and air-sea CO_2 flux, and cover the region from 15° N to 28° N and 88° W to 62° W. The gridded data and products are used for determination of status and trends of ocean acidification, for quantifying air-sea CO_2 fluxes, and for ground truthing models. Methodologies to derive the TA, pH and Ω_{Ar}, and to calculate the fluxes from fCO_{2w} temperature and salinity are described.

Introduction

Over the past 20 years a rapidly expanding program of measurements of surface water partial pressure of carbon dioxide (pCO_{2w})[1], or the fugacity of CO_2 (fCO_{2w})[1] has provided data to determine air-sea CO_2 fluxes and rates of ocean acidification on local to global scales (e.g. Boutin et al., 2008; Degrandpre et al., 2002; Evans et al. 2015; Schuster et al., 2012; Takahashi et al., 2014; Wanninkhof et al. 2019 a, b). Marginal seas, that historically had a dearth of measurements, have been targeted for increased observations. Through an industry, academic, and federal partnership between the U.S. National Oceanic and Atmospheric Administration (NOAA), Royal Caribbean Cruise Lines (RCCL), and the University of Miami, cruise ships were outfitted with automated surface water pCO_2 systems, also called underway pCO_2 systems (Pierrot et al., 2009). In 2002, the RCCL ship *Explorer of the Seas* (*EoS*) was equipped with an underway pCO_2 setup providing observations on alternating weekly transects from Miami, FL to the Northeastern and Northwestern Caribbean. In 2015, the *EoS* was repositioned out of the Atlantic and the *Celebrity Equinox* (*Eqnx*) was outfitted with an underway pCO_2 system. Additionally, an underway pCO_2 system was installed on the *Allure of the Seas* (*ALos*) in 2016. The *Eqnx* and *ALos* covered similar transects as the *EoS* but on more irregular and seasonal basis. A total of 582 cruises covered the region from 2002 through 2018. A map of all cruise tracks is shown in Figure 1. The number of cruises per year covering the Caribbean Sea and adjacent Western Atlantic are provided in Figure 2. There are fewer cruises in the middle part of the record when the *EoS* was diverted to other routes outside the area, and eventually repositioned.

[1] fCO_2 is the pCO_2 corrected for the non-ideal behavior of CO_2 (Weiss 1974). In surface water $fCO_{2w} \approx 0.997\ pCO_{2w}$

Deleted: provided
Deleted: at
Deleted: inorganic carbon system parameters
Deleted:
Formatted: Not Superscript/ Subscript
Deleted: ,
Deleted: ,
Formatted: Superscript
Formatted: Superscript
Deleted:
Deleted:
Deleted: (
Deleted:) E
Deleted: Western
Deleted: In 2008, the home port for *EoS* was shifted to Bayonne, New Jersey, and itineraries were shared between the Eastern Caribbean, Bermuda, and Eastern US. …
Deleted: *AoS*
Deleted: was outfitted with an underway pCO_2 system
Deleted: *AoS*
Formatted: Font: Not Bold
Formatted: Font: Not Bold
Deleted: bar graph shows

The surface water pCO_2 observational dataset and derived products including total alkalinity (TA), acidity (pH), aragonite saturation state (Ω_{Ar}), and air-sea CO_2 flux are of importance for determining the anthropogenic carbon uptake, and to assess trends and impacts of ocean acidification. The observational data are provided to the global surface ocean carbon atlas (SOCAT) (Bakker et al., 2016) and global CO_2 climatology (Takahashi et al., 2009; 2018). These data are the main source of fCO_2 observations available in the region, and the high frequency of measurements provides a seasonally resolved picture of changing fCO_{2w}. This effort has made the Northern Caribbean one of the few places in the world's ocean where such regional observational density has been established. The data and mapped products are interpreted in Wanninkhof et al. (2019b) who show large decadal changes in trends of surface water fCO_2 and associated changes in air-sea CO_2 fluxes.

The data from the first part of this record form the basis of the Caribbean ocean acidification product suite that maps ocean acidification conditions in the Caribbean (Gledhill et al., 2008; https://www.coral.noaa.gov/accrete/oaps.html; https://cwcgom.aoml.noaa.gov/erddap/griddap/miamiacidification.graph). The large, high quality, and well-resolved dataset is also used to validate models (Gomez et al., 2020).

For optimal application, datasets and associated data products are fully documented here, and are readily accessible according to the findable, accessible, interoperable and reusable (FAIR) principles (Wilkinson et al., 2016). The documentation of the cruises, the sampling methodology, and data reduction techniques are presented in brief. This is followed by a description of the approaches to calculate the different inorganic carbon system parameters. The procedure is to bin and average the fCO_{2w} on a 1˚ by 1˚ grid on monthly scales, referred to as gridded observations. Then the so-called second inorganic carbon system parameter is calculated that is used in conjunction with fCO_{2w}. We estimate the total alkalinity (TA) based on robust relationships of TA with salinity (Cai et al., 2010; Takahashi et al., 2014; Lee et al., 2006; Millero et al., 1998), and use a software program CO2SYS (Pierrot et al., 2006) to calculate the other inorganic carbon system parameters of interest, in this case pH and Ω_{Ar}. These data products are presented at monthly scales binned and averaged on a 1˚ by 1˚ grid, referred to as gridded products. Annual multi-linear regressions (MLR) are developed between the gridded fCO_{2w} data, and sea surface temperature (SST), sea surface salinity (SSS), location (latitude (Lat)and longitude (Lon)), and mixed layer depth as independent variables. These regressions are applied at monthly and 1˚ by 1˚ spatial resolution to the region between 15˚ N and 28˚ N, and 88˚ W and 62˚ W using remotely sensed or modeled independent variables, and used to calculated air-sea CO_2 fluxes. These calculated parameters are called gridded mapped products. The procedures and datasets, including an uncertainty analyses, and tables of column headers of the product created are provided below.

Deleted: surface water fCO_2 (
Deleted:)
Deleted: used
Deleted: 2018
Deleted: to estimate
Deleted: In this case w
Deleted: binned
Deleted:
Deleted: of interest
Deleted: -
Deleted: -
Formatted: Subscript
Deleted: ,
Deleted: detailed

1 Observations

The observational program is described in terms of the ships, voyages, and instrumentation. The ships predominantly sailed in the Caribbean Sea, but also had tracks outside the region, including in the Northeast of the USA, to Bermuda and in the Mediterranean. The description of operations, data, and products presented here cover the Northern Caribbean Sea and

Deleted: and

Western Atlantic, north of the Caribbean islands chain covering the region from 15° N to 28° N and -62° to -88° (= 62° W to 88° W) (Fig. 1). The homeports of the ships, where passengers embark and disembark, are Miami and Fort Lauderdale, FL. The *Explorer of the Seas (EoS*) changed homeport from Miami, FL to Cape Liberty Cruise Port, NJ in 2008, and changed its routes at that point to include cruises with Bermuda as a port of call. In 2015 the *EoS* was repositioned to the Pacific and the underway pCO_2 system was removed. From 2015 onward the *Celebrity Equinox (Eqnx)* and from 2016 onward the *Allure of the Seas* (*ALos)* covered the area. The *Eqnx* spent the summers of 2015 and 2016 in the Mediterranean, causing seasonal data gaps in the Caribbean.

1.2 Cruises

The *EoS* had 331 cruises from 2002 to 2015; the *Eqnx* completed 135 cruises from 2015 through 2018; and the *ALos* performed 116 cruises in the study area from 2016 through 2018. Temporal coverage over the 17 years shows at least bi-weekly occupations at the beginning of the record from 2002 to 2007, and at the end from 2014 through 2018, with fewer occupations in the years in between (Fig. 2). The cruises lasted between 7 and 14 days, and made about a half a dozen ports of call. The ships generally were in port from early morning to late afternoon, and transited between ports at night, except for long runs (e.g., from Miami to San Juan) when the ship sailed continuously for several days. Ports are listed in the metadata accompanying the original data.

The systems were installed in different locations for the three ships, but each had a dedicated seawater intake near the bow. The *EoS* had an intake in the bow thruster tube (≈3 m depth) that was non-optimal due to bubble entrainment during bow thruster operations and heavy seas. These observations have been culled from the datasets. The *ALos* and *Eqnx* had their intake at ≈5 m depth, but forward of the bow thruster and had fewer issues with bubble entrainment. On the *EoS*, the underway pCO_2 instrument was initially in a dedicated science laboratory built for purpose on the ship, and located amidships about 100 m from the intake. In 2008, a new system was placed in the engineering space closer to the bow with no apparent change in performance. For the *ALos* and *Eqnx*, the instruments were near the bow intake in the engineering space, about 5 m from the intake. The *EoS* had an air intake mounted on a mast at the forward most point of the main deck in August of 2008. The *Eqnx* had an air intake near the bow one level below the main deck since the initial installation in March 2015. The underway pCO_2 systems on these ships made marine boundary layer (MBL) air observations (xCO_{2a}) as described in Wanninkhof 2019b but these are not used in the data products presented. Typical cruise speeds were 22 knots which, with sampling every 2.5 minutes, yielded a fCO_{2w} sample approximately every 1.7 km except for 35 minutes every 4.5 hours when four calibration gases, and a CO_2-free reference gas were analyzed, followed by 5 atmospheric CO_2 measurements for the ships with air intakes. This created a gap of 24 km (≈1/4°) without fCO_{2w} measurements

Deleted: Northern Caribbean Sea and the Western Atlantic
Deleted: ,
Deleted: collectively called the Caribbean.
Deleted: ,
Deleted: *AoS*
Deleted: The underway pCO_2 systems were installed on three different ships of the Royal Caribbean Cruise Lines. …
Deleted: *AoS*
Deleted: The coverage represents the Northern Caribbean Sea and Western Atlantic, north of the Caribbean islands chain. …
Deleted: 16
Deleted: Figure
Deleted: Installation of t
Deleted: occurred
Deleted: the bow of the ship
Deleted:
Deleted: *AoS*
Deleted: also
Deleted: ve
Deleted: have
Deleted: *AoS*
Deleted: -
Deleted: Seawater flow to the systems was about 4 l min^{-1}.
Deleted: mounted in August of 2008
Deleted: thus
Formatted: Subscript

1.3 Instrumentation

1.3.1 pCO_2 system

The instrumentation is based on a community design described in Pierrot et al. (2009). The instruments were manufactured by General Oceanics Inc. and have performed to high accuracy specifications (Wanninkhof, 2013). The surface water drawn from the intake at about 4 l min^{-1} went through a 1.1 l sprayhead equilibrator with a water volume of 0.5 l and a headspace of 0.6 l. The spray and agitation caused the CO_2 in the headspace to equilibrate with the CO_2 in water with a response time of about 2 minutes (Pierrot et al., 2009; Web et al., 2016). Thus, the air in the headspace reached 99.8 % equilibration in 12 minutes. As the air is recirculated and surface waters were relatively homogeneous on hourly timescales, 100.0 % equilibration was assumed. The four calibration gases supplied by the global monitoring division of the environmental science research laboratory of NOAA (GMD/ ESRL/NOAA) were traceable to the WMO CO_2 mole fraction scale. The CO_2 concentrations of the standards spanned the range of surface water values encountered along the ship tracks (≈ 280- 480 ppm).

The gas entering the analyzer was dried by passing it through a thermo-electric cooler at 5˚ C and a PermaPure drier. The standards did not contain water vapor. The air and equilibrator headspace analyses typically had about 10 % or less humidity. Every 27 hours the CO_2 of LICOR model 6262 infrared analyzer were zeroed with the dry CO_2-free air and spanned with the highest standard. The water vapor channel was zeroed with the dry CO_2-free air but not spanned. The dry mole fraction of CO_2 (xCO_2 in parts per million, ppm), as calculated and output by the analyzer based on measured CO_2 and water vapor levels, were recorded. The systems were automatically turned off when the ships entered port, and upon shutdown they were back-flushed with fresh water removing particles from the inline water filter thereby alleviating clogging issues in the filter and reducing biofouling of water lines, filter and equilibrator.

Data from the *ALos* and *Eqnx* were transmitted to shore updated daily and displayed online in graphical format at https://www.aoml.noaa.gov/ocd/ocdweb/allure/allure_realtime.html and https://www.aoml.noaa.gov/ocd/ocdweb/equinox/equinox_realtime.html, respectively. These updates provided a near-real time opportunity to look at the response of surface water CO_2 to episodic events, such as passage of hurricanes, and yielded timely indications of instrument malfunction that could be remedied when the ships returned to port. The instruments have shown agreement to within 1 µatm with other state-of-art systems in intercomparison studies (Nojiri et al., Feb. 2009 pers. com.). Several different versions of the instrument have been deployed on the ships over the years but overall measurement principles and accuracies, estimated at better than 2 µatm (Pierrot et al., 2009; Wanninkhof et al., 2013), were maintained.

Deleted: are

Deleted: goes

Deleted: -

Deleted: -

Deleted: -

Deleted: causes

Deleted: will

Deleted: are

Deleted: can be

Deleted: under most circumstances

Deleted: Typical cruise speeds are 22 knots which, with sampling every 2.5 minutes, yields a sample approximately every 1.7 km except for 35 minutes every 4.5 hours when four calibration gases and a CO_2-free reference gas are analyzed, followed by 5 atmospheric CO_2 measurements for the ships with air intakes. This creates a gap of 24 km (≈1/4˚) without fCO_{2w} measurements. …

Moved (insertion) [8]

Moved (insertion) [7]

Deleted: them

Deleted: were bone dry

Deleted: ;

Deleted: both

Deleted: water

Formatted: Subscript

Deleted: as

Deleted: ,

Deleted: are

Deleted: are

Deleted: The fCO_{2w} levels are measured by infrared (IR) analysis of the headspace gas in the equilibration chamber. The gas in the headspace is partially dried (≈ >75%) before measurements. …

Deleted: The IR sensor (LI-COR 6262) is calibrated every 4.5 hours against four standard gases supplied by the global monitoring division of the environmental science research laboratory of NOAA (GMD/ ESRL/NOAA), traceable to the WMO CO_2 mole fraction scale. The CO

Moved up [8]: The CO_2 concentrations of the standards span the range of surface water values encountered along the ship tracks.

Deleted: have been

1.3.2 Thermosalinograph

Temperature and salinity were measured with a flow-through Seabird SBE45 thermosalinograph (TSG) that was in a seawater flow line parallel to the pCO_2 equilibrator. A SBE38 remote temperature probe was situated near the inlet before the pump, and was used as the SST measurement. The TSGs and temperature probes were maintained by collaborators from the Marine Technical group at the Rosenstiel School of Marine and Atmospheric Sciences at the University of Miami (RSMAS/U. Miami). The TSGs on the ships were factory calibrated on an annual basis. Post-calibrations showed no drift in the temperature sensor but occasionally some drift in the conductivity.

1.3.3 Other instrumentation

The underway effort is part of a larger scientific operation lead by RSMAS called Oceanscope (https://oceanscope.rsmas.miami.edu/). Additional instrumentation onboard the ships include the Marine-Atmospheric Emitted Radiance Interferometer (M-AERI) to assess surface skin temperature retrievals from a number of radiometers on earth-observation satellites (Minnet et al., 2001). The M-AERI's are Fourier-Transform Infrared interferometers situated on the deck viewing the sea surface away from the wake. Acoustic Doppler Current Profilers (ADCP) mounted on the hull of the ships are used to measure ocean currents.

2 Datasets

2.1 pCO_2 data

Full details on data acquisition with these systems and calculation of pCO_2 and fCO_2 can be found in Pierrot et al. (2009). Post-cruise, the xCO_2 data were processed by first linearly interpolating each standard measured every ~4 hours to the time of a sample measurement and then recalculating the air and water xCO_2 values based on the linear regression of the interpolated standard values at the time of sample measurement. For 3 cruises, the analyzer output showed negative water vapor values due to the condition of desiccant chemicals, and thus yielded erroneous dry xCO_2 values. Separate processing routines were developed to correct for these situations (available on request from D. Pierrot). The post-cruise corrected xCO_2 values were used for calculation of pCO_2 and fCO_2 as described in the calculation section.

2.2 Thermosalinograph, sea surface temperature and salinity data

The SST data were obtained from a temperature probe (Seabird, model SBE38) near the intake. The salinity was determined with a thermosalinograph (Seabird, model SBE45), from the measured conductivity and temperature in the unit using the internal software of the SBE45. The SST and SSS data were appended to the pCO_2 data records in real time and also logged

Deleted: are
Deleted: is
Deleted: is
Deleted: is
Deleted: thermosalinograph
Deleted: and swapped out annually for calibration.
Moved (insertion) [1]
Deleted: thermosalinographs
Deleted: ,
Deleted: used
Deleted: Briefly, the pCO_2 data was acquired at approximately 2.5 minute intervals in a continual sequence. The sequence included 4 reference standards spanning the range of surface water values (≈ 280- 480 ppm), 5 marine boundary layer (MBL) air measurements (for the ships with an air inlet), and 100 equilibrator headspace samples, henceforth called water samples. The full sequence took about 4.5 hours…
Moved up [7]: The gas entering the analyzer was dried by passing them through a thermo-electric cooler at 5˚ C and a PermaPure drier. The standards were bone dry; both air and water analyses typically had about 10 % or less humidity. Every 27 hours the LICOR model 6262 infrared analyzer was zeroed with the CO_2-free air and spanned with the highest standard. The dry mole fraction of CO_2 (xCO_2 in parts per million, ppm), as calculated and output by the analyzer based on measured CO_2 and water vapor levels, were recorded. Two weeks
Deleted: Two weeks of output data from the *AoS* and *Eqnx* are displayed online in graphical format at https://www.aoml.noaa.gov/ocd/ocdweb/allure/allure_realtime.html and https://www.aoml.noaa.gov/ocd/ocdweb/equinox/equinox_realtime.html, respectively….
Deleted: were
Deleted: Infrequently
Deleted: ed
Deleted: dried
Deleted: were

via another shipboard computer at more frequent intervals. The SSS data was not quality controlled and no corrections to the SSS data were made, other than removal of spikes and values that were out of range (<5 and > 40). As salinity has minimal effect on the calculated fCO_2, bad or missing salinities were removed and substituted by linearly interpolated values to eliminate gaps. When SST were not recorded in the CO_2 files or in error, the SST gaps were filled from the high resolution SST data files maintained by the RSMAS Oceanscope project. On the rare occasion (≈<0.1 %) that SST was not recorded at all, SST data was estimated from the equilibrator temperature data (T_{eq}) after applying a constant offset between T_{eq} and SST using SST data before and after the gap. On average the T_{eq} was 0.12 ± 0.28˚C lower than SST for all the cruises. Per cruise the standard deviation (stdev) of the difference of T_{eq} and SST was on the order of 0.04 ˚C. The in situ pCO_2 data calculated with T_{eq} was flagged with a WOCE quality control flag of 3 which refers to data that is deemed questionable and has a larger uncertainty.

For the regionally mapped products on a 1-degree grid and monthly timescale (1˚ by 1˚ by mo), SST and SSS were obtained from the following sources: The SSS data were from a numerical model, the Hybrid Coordinate Ocean Model (HYCOM) (https://HYCOM.org/) and referred to as SSS_{HYCOM}. The SST product for the region is the Optimum Interpolated SST, OISST from https://www.esrl.noaa.gov/psd/. (Reynolds et al., 2007). It uses data from ships, buoys and satellites to generate the fields. For the OISST the reference SST is from buoys, and the other SST data obtained from ships and other platforms were adjusted to the buoy data by subtracting 0.14˚C in the OISST product (Reynolds et al., 2007).

2.3 Wind speed data

Winds were measured on the ships but these data are not used as they are not synoptic for the whole region which is a requirement for the regional flux maps. Instead, wind speeds were obtained from the updated cross-calibrated multi-platform wind product (CCMP-2) (Atlas et al., 2011). The mean scalar neutral wind at 10 m height $<u_{10}>$, and its second moment $<u_{10}^2>$ were used to calculate the fluxes. They were determined from the ¼ degree, 6-hourly product that was obtained from Remote Sensing Systems (RSS) (www.remss.com). This product relies heavily on the European Center for Median Weather Forecasting (ECMWF) assimilation scheme that uses in situ and remotely sensed assets, particularly (passive) radiometers on satellites. The directional component uses scatterometer data. The ¼ degree, 6-hourly CCMP-2 product was binned and averaged in 1-degree grid boxes on monthly scales (1˚ by 1˚ by mo). In absence of CCMP-2 data for 2018, the wind product from European Reanalysis, ERA5, was used (https://www.ecmwf.int/en/forecasts/datasets/reanalysis-datasets/era5, Copernicus Climate Change Service, 2017). The ERA5 wind data are at 31-km and 3-hourly resolution but were binned and averaged in the same manner as the CCMP-2 winds. There were no apparent biases between the scalar winds for the two products in the Caribbean.

2.4 Mixed layer depth data

No MLD determinations were made on the cruises and limited observational estimates from other sources are available. The MLDs provided here are from the same numerical model (HYCOM) as used for the mapped SSS, and obtained from

Moved up [1]: The thermosalinographs on the ships were factory calibrated on an annual basis. Post-calibrations showed no drift in the temperature sensor but occasionally some drift in the conductivity. No

Deleted: The SST and salinity data, obtained from temperature and conductivity measured in the thermosalinograph, were appended to the pCO_2 data records in real-time and also logged via another shipboard computer at a more frequent interval. The thermosalinographs on the ships were factory calibrated on an annual basis. Post-calibrations showed no drift in the temperature sensor but occasionally some drift in the conductivity. No corrections to the sea surface salinity (SSS) were made and salinity did not undergo further quality control other than removal of spikes and values that were out of range.

Deleted: ,

Deleted:

Deleted: but p

Deleted: -

Deleted: as

Deleted: .

Deleted: whole

Deleted:

Deleted: in the OISST product

Deleted: -

Deleted:)

Deleted: (

Moved (insertion) [2]

Deleted: .

http://www.science.oregonstate.edu/ocean.productivity/index.php. The MLDs are based on a density contrast of 0.03 between surface and subsurface. Mixed layer depths (MLD) are used as an independent variable in the MLRs to map the fCO_{2w} values. They are also needed if mixed layer dissolved inorganic carbon (DIC) inventories are desired, and to determine the effect of mixed layer depth on the changes in fCO_{2w}. As shown in Wanninkhof (2019b, Figure 9), MLDs are negatively correlated with fCO_{2w}. They are provided in the gridded mapped product.

3 Calculations

The calculations of the concentrations and fluxes follow standard procedures as described below. The mapping procedures are detailed. The section on uncertainty includes an example of different possible means of mapping and the effect on the final product.

3.1 Calculation of pCO_2

The starting point in the calculations, which were aided by use of MATLAB routines following the procedures as in Pierrot et al. (2009), were calibrated (dry) xCO_2.

The xCO_2 values were converted to pCO_{2eq} (µatm) values:

$$pCO_{2eq} = xCO_{2eq} (P_{eq} - pH_2O) \quad (1)$$

where eq refers to equilibrator conditions. The P_{eq} is the pressure in the equilibrator headspace and pH_2O is the water vapor pressure calculated according to Eq. 10 in Weiss and Price (1980). The pCO_{2eq} was corrected to surface water values using the intake temperature (SST) and the temperature of water in the equilibrator (T_{eq}) according to the empirical relationship that Takahashi et al. (1993) developed for North Atlantic surface waters:

$$pCO_{2w} = pCO_{2eq}\, e^{(0.0423(SST-Teq))} \quad (2)$$

This empirical correction for temperature is widely used but it is of note that applying the thermodynamic relationships for carbonate dissociation constants yields different temperature dependencies that are a function of temperature. For average SST in the Caribbean of 27.0 ˚C the coefficient of temperature dependence varies from 0.036 to 0.040 using commonly used constants as provided in inorganic carbon system programs such as CO2SYS (Pierrot et al, 2006) compared to the coefficient of 0.0423 (or 4.23 % $˚C^{-1}$) used above. On average the difference between SST and T_{eq} is 0.12 ˚C for all the cruises such that the correction from T_{eq} to SST using the coefficient of 0.0423 in Eq. 2 is 1.9 µatm under average conditions of SST= 27 ˚C and fCO_{2w} =374 µatm. Using a temperature coefficient of 0.036 the temperature correction would be 1.6 µatm, or a 0.3 µatm difference.

3.2 Calculation of fCO_2 in air and water

The fCO_2 is the pCO_2 corrected for non-ideality of CO_2 solubility in water using the virial equation of state (Weiss, 1974). The correction can be expressed as: $fCO_{2a,w} = e^{g(SST,P)}\, pCO_{2a,w}$

Deleted:

Deleted: are not necessary to calculate the parameters in the datasets but they …

Deleted: interpolate

Deleted: therefore provided

Deleted: in the mapped data products. No MLD determinations were made on the cruises and limited observational estimates from other sources are available. The MLDs provided here are from the same numerical model (HYCOM) as used for the mapped SSS and obtained from http://www.science.oregonstate.edu/ocean.productivity/index.php. The MLDs are based on a density contrast of 0.03 between surface and subsurface, and are only provided …

Moved up [2]: . No MLD determinations were made on the cruises and limited observational estimates from other sources are available. The MLDs provided here are from the same numerical model (HYCOM) as used for the mapped SSS and obtained from http://www.science.oregonstate.edu/ocean.productivity/index.php. The MLDs are based on a density contrast of 0.03 between surface and subsurface, and are only provided in the

Deleted: (1˚ by 1˚ by mo)

Deleted: ,

Deleted: with an example of different possible means of mapping and the effect on the final product…

Deleted: are

Deleted: are

Deleted: values that were referenced against four gas standards covering the range of measurements. Standards were supplied by

Deleted: Standards were supplied by GMD/ ESRL/NOAA, traceable to the WMO CO_2 mole fraction scale.…

Deleted: using

Deleted: –

Deleted: =

Deleted: sampled

Deleted: for

and:

$$g(T,P)=[(-1636.75+12.0408T-0.0327957T^2+0.0000316528T^3)+2(1-xCO_2\,10^{-6})^2\,(57.7-0.118T)\,(P/1013.25)]/(82.0575T) \quad (3)$$

where T is in Kelvin, xCO_2 in is ppm, and P is in mbar.

Under average conditions in the Caribbean, the function $e^{g(SST,P)} \approx 0.997$ and fCO_{2w} will be ≈ 1.2 µatm less than pCO_{2w}. As the corrections from partial pressure to fugacity in air and water are approximately the same, the difference between ΔpCO_2 (=pCO_{2w}-pCO_{2a}) and ΔfCO_2 (=fCO_{2w}-fCO_{2a}), that were used to determine the fluxes (Eq. 5), is negligible (≈<0.1 µatm).

3.3 Gridding procedure

Gridding of the observations of fCO_{2w}, SST, and SSS was performed by binning and averaging the data in (1˚ by 1˚ by mo) cells. At typical ship speeds of 22 knots, the ship covered 1˚ in about 2.5 hours taking 60 measurements. This would yield about 250 measurements per month assuming weekly cruises through the area. The actual number of measurements per grid cell ranged from 8 to 500. The higher number of observations per cell were mostly in the latter part of the record, when the *Eqnx* and *ALos* operated in the same area. The total number of observations from March 2002 through December 2018 was 1.13 million, and the total number of (1˚ by 1˚ by mo) grid cells with observations was 9224.

The gridding facilitated the co-location and merging of products such as MLD_{HYCOM}, SSS_{HYCOM}, OISST, $\langle u^2 \rangle_{CCMP}$, and Marine Boundary Layer (MBL) xCO_2, xCO_{2MBL} into the gridded observational dataset for further interpretation. The gridded data aided comparison of *in situ* SST with OISST and SSS with SSS_{HYCOM}. The average difference between SSS and SSS_{HYCOM} for the 2002-2018 data was -0.1 ± 0.28 (n= 9224), and for SST and OISST the difference was 0.25 ± 0.40 ˚C (n= 9224) with the in situ SSS being lower and SST being higher. While both differences include zero within their standard deviation, the temperature difference is in agreement with expected cooler near-surface temperatures that could lead to lower fCO_{2w} which, in turn, have a large impact on the calculated air-sea fluxes.

3.4 Mapping procedures for fCO_{2w} and fluxes

3.4.1 Mapping fCO_{2w} using a multi-linear regression

The gridded observations (1˚ by 1˚ by mo) represented about 10 % of the area and months of investigation from 15 to 28 ˚N and 88 to 62 ˚W over the period of investigation. To interpolate ("map") the data in space (334 grid cells) and time (192 months) a multi-linear regression (MLR) approach was used to determine fCO_{2w} in each grid cell. For each year from 2002 through 2018 the gridded fCO_{2w} observations were regressed against the 1-degree monthly gridded values of position (Lat and Lon), SST, MLD, and SSS. Other permutations of independent parameters were tested but yielded less robust fits (see Appendix A). Annual MLRs were created as fCO_{2w} levels change over time in response to increasing atmospheric CO_2 levels. If fCO_{2w} kept pace with atmospheric CO_2 increase this would translate to a linear trend of fCO_{2w} of 2.13 µatm yr^{-1} over the time period. As shown in Wanninkhof et al. (2019b), multi-year (>4-yr intervals) trends varied from -4 to 4 µatm yr^{-1}, with an average linear trend in fCO_{2w} of 1.4 µatm yr^{-1} from 2002-2018.

Deleted: are were used to determine the fluxes (Eq. 4 ... [1]

Deleted: **3.3 Calculation of fluxes** ¶
For the determination of the air-sea CO_2 flux (F_{CO2}, mol m^{-2} yr^{-1}), a bulk formulation is applied to the data from the gridded mapped product:¶
→ $F_{CO2} = k\ s\ \Delta fCO_2$ →→→→→→→→→→→→ (4)¶
where ΔfCO_2 is (fCO_{2w}-fCO_{2a}), s is the seawater CO_2 solubility (Weiss and Price, 1980), and k is the gas transfer velocity parameterized as a function of wind speed (Wanninkhof, 2014): ¶
→ $k = 0.251 \langle u_{10}^2 \rangle (Sc/660)^{-1/2}$ →→→→→→→→→→ (5)¶
where $\langle u_{10}^2 \rangle$ is the monthly 2nd moment of the wind speeds reported in CCMP-2. The 2nd moment accounts for the impact of variability of the wind speed on k. It is determined by taking the monthly average of the sum of squares of the wind speed in CCMP-2 provided at 6-hours and ¼˚ grid resolution. The number of wind speed observation in a 1˚ by 1˚ by mo grid is 1920. This sample density captures the frequency spectrum of winds except that extreme wind events such as hurricanes are not fully represented due to the local nature of the extremes and inherent smoothing in the CCMP-2 product. The Sc is the Schmidt number of CO_2 in seawater, defined as the kinematic viscosity of seawater divided by the molecular diffusion coefficient of CO_2. It is determined as a function of temperature from Wanninkhof (2014). At the average temperature of 27 ˚C the Sc_{CO2} equals 475. Over the typical range of SST in the Caribbean from 24 ˚C to 30 ˚C, the $(Sc/660)^{-1/2}$ will vary from 1.1 to 1.27, indicating that the gas transfer velocity will be 27 % higher at an SST of 30 ˚C compared to a SST of 20 ˚C that would correspond to a Sc of 660.¶

Deleted: **4 … Binning** ... [2]

Deleted: Binning Gridding of the observations of fCO_{2w}, SST, and ... [3]

Deleted: gridding gridding facilitates ... [4]

Formatted: Subscript

Deleted: $_{MBL}$ into the gridded observational dataset for further ... [5]

Moved (insertion) [4]

Deleted: 5

Formatted: Normal

Formatted: Subscript

Deleted: ¶ ... [6]

Formatted ... [7]

Deleted: At steady state this increase would raise fCO_{2w} by 2.13 µatm yr^{-1} over the time period but the observed…

Moved (insertion) [3]

Deleted: 2018 in(…Wanninkhof et al., …(2019b)).… multi-year ... [8]

Moved up [3]: 2018 (Wanninkhof et al., 2019b).

The annual MLRs were created of the form:

$$fCO_{2w} = a\,Lon + b\,Lat + c\,OISST + d\,MLD_{Hycom} + e\,SSS_{Hycom} + f \quad (4)$$

with the coefficients for each year, along with the standard error in fCO_{2w} and standard error in each of the coefficients provided in Table 1. The standard error in the fCO_{2wMLR} ranged from 5 to 9 µatm for each year. Using the locations, OISST (the optimal interpolated SST product), MLD_{Hycom} and the SSS_{Hycom} (output of the HYCOM model) the fCO_{2MLR} is determined for each grid cell. There were significant cross-correlations between independent variables such that effect of the, often significant, year-to-year differences in coefficients were difficult to interpret. However, the fCO_{2wMLR} from the annual MLRs faithfully reproduced the trends and variability.

The MLRs were produced for each year such that the mapped products could be extended for future years in a straightforward fashion. To determine if there were anomalous discontinuities between subsequent annual MLRs that could impact the timeseries, the difference in between fCO_{2w} for subsequent months were plotted versus time in Figure 3. No significant discontinuities were observed between December and January. Only for December and January 2008/2009, 2009/2010, and 2016/2017 there appear to be slight differences in the pattern of monthly progressions but such anomalies are observed during other times of year as well. Using an MLR that includes year as one of the coefficients (supplemental material S2 and S3) provides a slightly worse fit. Moreover, using such a fit would necessitate recalculating the mapped products every time a new year is added.

As illustration of differences between gridded and mapped products the results of the fCO_{2wMLR} calculated with the MLRs for 2004, 2011, and 2017 (Table 1) are plotted in Figure 4a along with the gridded observations for the grid cells that span the longitude range from 88°W to 62° W between 23° N and 24° N (see Fig.1). Figure 4a shows that the mapped product using annual MLRs show the increases in fCO_{2w} over time in the region, and consistent differences in patterns between the East and the West for the three years. The mapped product showed a reasonable correspondence with the gridded observations. Some of the differences between the gridded observations and mapped product were caused by the mismatch between SST and SSS *in situ* with the OISST and SSS_{HYCOM} (Figs. 4b and 4c). In particular, the strong minima in OISST at 79° W is not seen in the SST. This is likely because the OISST captured the lower SST near the coast of Cuba. This caused the fCO_{2wMLR} product to be lower as well, as shown in Figure 4a. It illustrates that the mapped fCO_{2wMLR} product is both influenced by the annual MLR, and the gridded MLD_{Hycom}, OISST, and SSS_{Hycom}.

Deleted: have the form of
Deleted:
Deleted:
Deleted:
Deleted: 6
Formatted: Subscript
Formatted: Subscript
Deleted: →→
Formatted: Subscript
Formatted: Subscript
Formatted: Subscript
Deleted: The coefficients for each year, along with the error in fCO_{2w} and uncertainties in each of the coefficients are shown in Table 1. The error in the calculated fCO_{2w} ranges from 5 to 9
Deleted: The strongest dependence was with SST.
Deleted: are
Deleted: As illustration, the results of the MLRs for 2004, 2011, and 2017 (Table 1) were applied to the January data in 2004, 2011, and 2017 and are plotted in **Figure 3a** along with the observations (if available) for the grid boxes that span the longitude range from 88˚W to 62˚ W between 23˚ N and 24˚ N (see Figure 1). **Figure 3a** shows that the mapped product using annual MLRs reflected the increases in fCO_{2w} in the region, and consistent differences in patterns between the East and the West for the three years. The mapped product showed a reasonable correspondence with the gridded observations. Some of the deviations between the gridded observations and mapped product were caused by the mismatch between SST and SSS *in situ* with the OISST and SSS_{HYCOM} (**Figures 3b and 3c**). In particular, the strong minima in OISST at 79˚ W were likely due to the OISST capturing the lower SST near the coast of Cuba. This caused the mapped fCO_2 product to be lower as well, as shown in Figure 3a. It illustrates that the gridded fCO_2 product is both influenced by the annual MLR, and the MLD, SST, and SSS products used for mapping.…
Formatted: Font: Not Bold
Formatted: Font: Not Bold
Formatted: Font: Not Bold
Formatted: Font: Not Bold
Formatted: Font: Not Bold
Formatted: Font: Not Bold
Formatted: Font: Not Bold
Formatted: Subscript
Formatted: Subscript

3.4.2 Determining the air-sea CO_2 fluxes for the region

For the determination of the air-sea CO_2 flux (F_{CO2}, mol m^{-2} yr^{-1}), a bulk formulation was applied using the gridded mapped product:

$$F_{CO2} = k\, K_0\, \Delta fCO_2 \quad (5)$$

where ΔfCO_2 is (fCO_{2w}-fCO_{2a}), K_0 is the seawater CO_2 solubility that is a function of temperature and salinity (Weiss and Price, 1980), and k is the gas transfer velocity parameterized as a function of wind speed (Wanninkhof, 2014):

$$k = 0.251 <u_{10}^2> (Sc/660)^{-1/2} \quad (6)$$

where $<u_{10}^2>$ is the monthly 2nd moment of the wind speeds reported in CCMP-2. The 2nd moment accounts for the impact of variability of the wind speed on k. It is determined by taking the monthly average of the sum of squares of the wind speed in CCMP-2 provided at 6-hours and ¼° grid resolution. The number of wind speed observation in a (1° by 1° by mo) grid is 1920. This sample density captures the frequency spectrum of winds in the grid boxes except that extreme wind events such as hurricanes are not fully represented due to the local nature of the extremes and inherent smoothing in the CCMP-2 product. The Sc is the Schmidt number of CO_2 in seawater, defined as the kinematic viscosity of seawater divided by the molecular diffusion coefficient of CO_2. It is determined as a function of temperature from Wanninkhof (2014). At the average temperature of 27 ˚C the Sc_{CO2} equals 475. Over the typical range of SST in the Caribbean from 24 ˚C to 30 ˚C, the $(Sc/660)^{-1/2}$ will vary from 1.1 to 1.27, indicating that the gas transfer velocity will be 27 % higher at an SST of 30 ˚C compared to a SST of 20 ˚C that would correspond to a Sc of 660.

The annual fCO_{2MLR} and modeled and remote sensed products, OISST, MLD_{HYCOM}, SSS_{HYCOM}, were determined for all (1° by 1° by mo) grid cells. The monthly fCO_{2aMBL} values were derived from the weekly average xCO_{2aMBL} of the stations on Key Biscayne (KEY) and Ragged Point Barbados (RPB) (CarbonTracker Team, 2019; https://www.esrl.noaa.gov/gmd/ccgg/flask.php). The second moments of the scalar winds, $<u^2>$ from CCMP-2 were averaged on the same grids. As no CCMP-2 product was available in 2018, the ERA5 wind product was used for the last year of the record.

Table 1. Coefficients for the MLR for each year *

	a (LON)	b (LAT)	c (SST)	d (MLD)	e (SSS)	f (Icept)	Standard error $fCO_{2w,MLR}$	r^2	#points
2002	-0.32	0.45	10.29	-0.04	0.77	24.4	4.72	0.90	537
	0.04	*0.11*	*0.18*	*0.02*	*0.72*	*25.8*			
2003	-0.56	0.32	9.24	-0.09	1.11	32.6	5.21	0.86	731

Deleted: ¶
Formatted: Subscript
Formatted: Subscript
Moved up [4]: 3.5 Mapping procedures for fCO_{2w} and fluxes¶
Deleted: Despite the large number of observations and monthly 1° by 1°gridding, only about 10% of the grid boxes had observations so some means of temporal and spatial interpolation was necessary. Therefore, t…
Formatted: Subscript
Deleted: Rs
Deleted: were used for the mapped products. From the
Deleted: that were
Deleted: available
Deleted: , a corresponding fCO_{2w} was determined
Deleted: For the air-sea CO_2 fluxes, t
Deleted: As noted in Atlas et al. (2011) the ERA5 winds are a part of the ECWFM wind products that are used as a prior in the CCMP-2, and thus scalar winds between products are very similar.…
Deleted: Error

	0.03	*0.09*	*0.17*	*0.02*	*0.66*	*24.6*			
2004	-0.42	0.82	10.34	-0.20	2.78	-55.4	5.21	0.92	740
	0.03	*0.09*	*0.17*	*0.01*	*0.63*	*23.6*			
2005	-0.43	0.49	8.71	-0.07	7.30	-172.0	6.58	0.85	664
	0.04	*0.12*	*0.18*	*0.02*	*0.85*	*32.1*			
2006	-0.31	1.13	9.60	-0.19	2.56	-26.6	4.99	0.89	670
	0.03	*0.08*	*0.16*	*0.02*	*0.70*	*26.1*			
2007	-0.62	1.12	10.56	-0.36	2.75	-77.8	7.04	0.79	483
	0.05	*0.15*	*0.32*	*0.03*	*1.33*	*49.0*			
2008	-0.12	1.12	10.58	-0.30	3.16	-55.8	5.66	0.95	107
	0.43	*0.31*	*0.45*	*0.05*	*1.39*	*59.8*			
2009	-0.66	0.30	7.18	-0.47	0.11	131.9	6.91	0.84	125
	0.22	*0.24*	*0.53*	*0.07*	*1.49*	*58.8*			
2010	-0.53	2.02	8.48	-0.23	2.12	-10.5	9.31	0.85	323
	0.17	*0.26*	*0.41*	*0.05*	*1.48*	*51.7*			
2011	-0.32	0.98	6.65	-0.28	3.06	46.8	7.19	0.76	305
	0.13	*0.19*	*0.34*	*0.04*	*1.51*	*59.7*			
2012	-0.13	1.66	10.81	-0.33	5.56	-154.1	7.29	0.91	358
	0.10	*0.16*	*0.28*	*0.04*	*1.36*	*50.9*			
2013	-0.43	1.30	11.45	-0.47	4.45	-137.5	8.16	0.83	219
	0.18	*0.23*	*0.48*	*0.05*	*1.63*	*55.5*			
2014	-0.60	0.62	9.48	-0.18	3.26	-45.2	7.02	0.78	362
	0.08	*0.15*	*0.29*	*0.03*	*1.06*	*37.7*			
2015	-0.84	0.14	7.76	-0.18	1.20	70.0	6.01	0.82	455
	0.04	*0.11*	*0.27*	*0.02*	*0.90*	*34.5*			
2016	-0.79	0.37	8.72	-0.14	4.17	-62.7	6.66	0.82	1001
	0.03	*0.08*	*0.20*	*0.01*	*0.45*	*17.1*			
2017	-0.42	0.56	9.49	-0.22	5.65	-112.6	6.17	0.87	974
	0.03	*0.08*	*0.15*	*0.02*	*0.58*	*17.1*			
2018	-0.34	-0.09	10.85	-0.13	6.24	-151.2	5.08	0.90	1162
	0.02	*0.07*	*0.13*	*0.01*	*0.39*	*14.7*			

* These annual regressions were used to create the mapped $fCO_{2w_{MLR}}$ fields using the 1° by 1° by month gridded data product. $fCO_{2w_{MLR}}$ = a Longitude + b Latitude + c OISST + d MLD_{Hycom} + e SSS_{Hycom} + f

The second row (in italics) for each annual entry is the error of the coefficient.

3.5 Gridded and mapped products for Alkalinity and pH_T

Total Alkalinity (TA) was determined from salinity. For estimation of TA several algorithms have been developed with salinity (Fig. 5) (Millero et al., 1998; Lee et al., 2006; Takahashi et al., 2014 and Cai et al., 2010). The relationship of Cai et al. 2010 , TA= 57.3SSS+ 296.4, stdev = 5.5 was used as this was determined from observations that are similar to the conditions in the Caribbean.

The pH_T, the pH on the Total scale at SST, was subsequently determined from the calculated TA and fCO_{2w}. For the gridded products the gridded SST and SSS were used to determined TA. For the pH_T the gridded TA and fCO_{2w}. were used. For the mapped products the gridded OISST and SSS_{Hycom} were applied in the calculations. The pH_T was calculated using the program CO2SYS for Excel V2.2 (Pierrot et al., 2006) with the apparent CO_2 dissociation constants, K_1, K_2 from Lueker et al. (2000); the KSO_4^- dissociation constants from Dickson (1990); thr KF dissociation constants from Perez and Fraga (1987); and the total boron relationship with salinity from Uppström (1974).

3.6 Aragonite saturation state (Ω_{Ar})

The aragonite saturation state (Ω_{Ar}) indicates the level of supersaturation or undersaturation of seawater with respect to the mineral aragonite, a polymorph of calcium carbonate, and part of the skeletal structure of many marine calcifiers. That is, when Ω_{Ar} is less than 1 aragonite dissolution is thermodynamically favored and when Ω_{Ar} is greater than 1 it has a tendency to precipitate. It is used as an indicator of ecosystem health with regards to ocean acidification (Mollica et al., 2018). In warm tropical regions surface water saturation states are well above one but no active precipitation takes place except under unusual circumstances in shallow waters, in a precipitation process called whitings (Purkis et al., 2017). The Ω_{Ar} is not measured directly and is defined as the product of calcium and carbonate ion concentrations divided by the solubility product of aragonite:

$$\Omega_{Ar} = [Ca^{2+}]\,[CO_3^{2-}]\,(K_{Ar}{}'_{sp})^{-1} \quad (7)$$

where $[Ca^{2+}]$ is the total calcium concentration and is derived from salinity: $[Ca^{2+}]$ = 0.02128 / 40.087 * (SSS/ 1.80655) = 293.84 S in mol/kg-SW (Riley and Tongudai, 1967). $[CO_3^{2-}]$ is the total carbonate ion concentration determined from two of the inorganic carbon system parameters, and $K_{Ar}{}'_{sp}$ is the apparent solubility product of aragonite in seawater at a specified

Deleted: for each year
Deleted: ,Mapped
Formatted: Subscript
Formatted: Subscript
Deleted: 6
Deleted: Determination of
Deleted:
Deleted: Alkalinity and mapping of pH
Formatted: Subscript
Deleted: ¶
Formatted: Subscript
Formatted: Subscript
Formatted: Subscript
Formatted: Subscript
Formatted: Subscript
Deleted: Several algorithms have been developed (Millero et al., 1998; Lee et al., 2006; Takahashi et al., 2014 and Cai et al., 2010) that show close agreement for the conditions in the Caribbean. Figure 4 shows several TA-salinity relationships over the salinity range encountered in the region along with error bars for the Cai et al. (2010) relationship depicting the uncertainty of 5.5 µmol kg^{-1}. The relationship of Cai et al. (2010), specifically developed for the Caribbean Sea (see insert of Figure 10 in Cai et al., 2010), TA= 57.3SSS+ 296.4, stdev = 5.5 was used here. …
Deleted: As shown in Figure 4 the agreement between relationships was good, and choice of TA relationship did not have a determining influence on results. The calculated TA was used to determine pH with the gridded fCO_{2w} product. The program CO2SYS for excel V2.2 (Pierrot et al., 2006) was used with the apparent CO_2 dissociation constants, K_1, K_2 from Lueker et al. (2000); KSO_4^- dissociation constants from Dickson (1990); KF dissociation constants from Perez and Fraga (1987); and Total Boron salinity relationship from Uppström (1974). The pH product was determined at the OISST and on the total scale (pH_T) on the 1° by 1° by mo grid.¶
This approach of calculating the pH from the monthly product differs from other created pH products (Lauvset et al., 2016; Jiang et al., 2015) where the pH is calculated from the in situ measurements of DIC and TA and then regressed and gridded. To examine the differences derived from using one or the other approach, both wer… [9]
Deleted: 7
Deleted: ,
Deleted: Values of Ω_{Ar} that are less than one indicate that aragonite would dissolve, and greater than one it would have a tendency to… [10]
Deleted: s
Deleted: 8
Deleted: where $[Ca^{2+}]$ is the total calcium concentration and is derived from salinity: $[Ca^{2+}]$ =293.86 S (Millero 1995)…
Deleted: four measured

salinity, temperature and pressure. In this work [CO_3^{2-}] was determined from the gridded fCO_{2w} and calculated TA using the CO2SYS program. For surface waters, $K_{Ar}'_{sp}$ is

$$pK_{Ar}'_{sp} = -[-171.945 - 0.077993\,T + 2903.293/T + 71.595\log(T) + (-0.068393 + 0.0017276\,T + 88.135/T)\,S^{0.5} - 0.10018\,S + 0.0059415\,S^{1.5}] \quad (8)$$

Where $pK_{Ar}'_{sp} = -\log K_{Ar}'_{sp}$, T is temperature in Kelvin (K), and S is salinity (Mucci,1983). As with pH_T, the Ω_{Ar} gridded product was determined from the gridded (1˚ by 1˚ by mo) values of SSS, SST, fCO_{2w} and TA, while the mapped product uses SSS_{Hycom}, OISST, fCO_{2wMLR} and TA.

3.7 Uncertainty of observations, gridded and mapped products

The uncertainty of the products is difficult to quantify due to the many factors, calculations, and interpolations influencing the overall uncertainty. Moreover, the uncertainty estimate includes a random and a systematic component. The latter can have a large influence on interpretations, particularly on the calculated air-sea CO_2 fluxes. Below we address the uncertainty in terms of standard errors in the observations; in the gridded products; and in the mapped products. For the calculated quantities and nomenclature we follow the approach in Orr et al. (2018). The standard uncertainty is characterized by its standard deviation/error of the measured quantities and the standard uncertainties of the input variables. The propagated uncertainty of a calculated variable is called the combined standard uncertainty. Error propagation for addition is $(e_A^2 + e_B^2 + \ldots.)^{0.5}$ and for multiplication it is $((e_A/A)^2 + (e_B/B)^2 + \ldots.)^{0.5}$, where A and B are the variables, and e_A is the standard error in variable A.

The individual measurements of fCO_{2w} have a combined standard uncertainty of less than 2 µatm based on a propagation of error of instrument response, equilibrator efficiency standardization, and temperatures and pressures at equilibration and at the sea surface (Pierrot et al., 2006). The performance and output data from the UWpCO_2 systems have been checked at manufacturer, in intercomparison exercises, and at sea. SST measurements, at point of measurement, are accurate to 0.02 ˚C and SSS to 0.1 based on instrument specifications and annual calibrations.

The combined standard uncertainty in gridded product will vary based on the number of measurements. It includes the actual variability in the 1˚ by 1˚ cells. To estimate the uncertainty per grid cell, the stdev of the fCO_{2w} in each cell was determined and then the average of the stdev for the 9924 cells with observations was taken. The average stdev was 3.4 ± 2.6 µatm (n=9224). The same procedure was followed for SST and SSS and yielded values of 0.22± 0.19 ˚C for SST; and 0.10± 0.10 for SSS. These were relatively small uncertainties compared to the monthly spatial range of ≈ 20 µatm for fCO_{2w}; ≈1 ˚C for

Deleted: monthly binned
Deleted:
Deleted:
Deleted:
Deleted: A1
Formatted: Superscript
Deleted: 9
Deleted: mapped
Deleted: .
Formatted: Subscript
Formatted: Subscript
Formatted: Superscript
Formatted: Subscript
Formatted: Superscript
Formatted: Subscript
Formatted: Superscript
Formatted: Superscript
Formatted: Not Superscript/ Subscript
Formatted: Not Superscript/ Subscript
Formatted: Not Superscript/ Subscript
Formatted: Subscript
Formatted: Subscript
Formatted: Subscript

SST; ≈1 in SSS. The amplitude of the seasonal cycle of ≈40 µatm for fCO_{2w} and ≈4 ˚C for SST were significantly greater than the standard uncertainties as well.

The calculated parameters for the gridded products, TA, pH_T and Ω_{Ar} have an added uncertainty due to the uncertainty in the constants and parameterizations. The agreement between TA-SSS relationships was good, and choice of TA relationship did not have a determining influence on results. We used TA=57.3 SSS_OBS + 296.4 specifically developed for the Subtropical Western Atlantic (see insert of Figure 10 in Cai et al., 2010). The standard error for the relationship was 5.5 µmol kg^{-1}. The average stdev for salinity in the grid cells is 0.1 which translates in a uncertainty gridded TA of 5.8 µmol kg^{-1}. Thus combined standard uncertainty for TA is $((5.5/2375)^2+(5.8/2375)^2)^{0.5}$ 2375 = 8 µmol kg^{-1}, where 2375 µmol kg^{-1} is the average TA.

pH_T is determined from fCO_{2w} and calculated TA with associated uncertainties. An added uncertainty for the calculated pH_T is the uncertainty in the dissociation constants that are used to calculate pH_T . These uncertainties can be calculated using a modified version of CO2SYS (Orr et al. 2018). As shown in Orr et al. (2018, Figure12), the uncertainty in the constants dominates the calculated pH_T. Using the uncertainty in the constants as presented in the program, an uncertainty of gridded TA of 8 µmol kg^{-1} and 3.4 µatm for fCO_2 yields an combined standard uncertainty in pH of 0.0075. For comparison the uncertainty in pH would be 0.0070 if state-of-the art measurement uncertainties in TA of ±3 µmol kg^{-1} and ±2 µatm for fCO_2 are used. Similarly, the uncertainty Ω_{Ar} using the same approach and uncertainties in independent parameters is ±0.20. Again it is the uncertainty in the dissociation constants that dominate the overall uncertainty.

For the mapped products there is the additional uncertainty through the use of regressions. The standard errors of the annual regressions in fCO_{2wMLR} and the coefficients of the independent parameters are provided in Table 1. The average standard error for the fCO_{2wMLR} for the 17 years is 6.4 ± 1.2 µatm. Following the approach above for the other independent parameters and propagating these uncertainties yields a combined standard uncertainty of 0.0090 in mapped pH and 0.21 in mapped Ω_{Ar}

Systematic errors are introduced by the different SST and SSS data that are used for the gridded and mapped products, with the former using the gridded measured SST and SSS, and the latter the SSS_{Hycom} and OISST products. The magnitude of the systematic uncertainty between the mapped and gridded product is estimated from the difference in the gridded and mapped parameters for cells that have both gridded and mapped products (Table 2). Another possible source of systematic uncertainty is using the gridded and mapped fCO_{2sw}, SSS, and SST to calculate the TA, pH_T and Ω_{Ar} rather than using the in situ values to calculate the parameters and then gridding them. This uncertainty is small based on the low uncertainty of variables in each cell as shown from their stdev provided in the gridded products (Table 3).

Formatted: Subscript
Formatted: Superscript
Formatted: Superscript
Formatted: Superscript
Formatted: Not Superscript/ Subscript
Formatted: Font: (Default) Times New Roman, Font color: Auto
Formatted: Subscript
Formatted: Subscript
Formatted: Subscript
Formatted: Subscript
Formatted: Font: (Default) +Body (Times New Roman), Font color: Black
Formatted: Subscript
Formatted: Subscript
Formatted: Subscript
Formatted: Subscript
Formatted: Subscript

This is confirmed by comparing this method with the approach of calculating the pH and then gridding and mapping as done in Lauvset et al. (2016) and Jiang et al. (2015). To examine the differences derived from using one or the other approach, both were compared for 2017 data. The pH and TA were calculated for every fCO_{2w} observation and binned into a (1˚ x 1˚ x mo) grid. A MLR was from the calculated pH created for 2017:

$$pH_T(\pm 0.005) = 0.0003194\ Lon - 0.00046744\ Lat - 0.00965183\ SST + 0.00019602\ MLD + 0.00069378\ SSS + 8.3240 \qquad r^2 = 0.89\ (n = 1244) \qquad (9)$$

This MLR was then applied to the independent variables for each grid box to determine $pH_T(MLR)$. This was compared to the approach used here of calculating the pH using the mapped fCO_{2wMLR} and TA-SSS relationships on (1˚ x 1˚ x mo) grids, called $pH_T(fCO_{2w},TA)$. The two approaches provided similar results with $pH_T(fCO_{2w},TA) - pH_T(MLR) = -0.0001 \pm 0.005$ for 2017. The small difference showed a pattern with SST (Fig. 6) but not with the other independent variables. The differences using either $pH_T(fCO_{2w},TA)$ or pH_{T_MLR} are an order of magnitude smaller than the combined standard uncertainties such that the approach of using mapped fCO_{2w} and TA to determine $pH_T(MLR)$ yielded precise and consistent gridded pH_T.

Calculated air-sea CO_2 fluxes have a significant uncertainty as they are driven by relatively small air-water concentration differences. Using the uncertainty in fCO_{2wMLR} of 6.4 µatm and an uncertainty fCO_{2a} of 1 µatm, and uncertainties in k of 20 % (Wanninkhof, 2014) and K_0 of 0.002 (Weiss, 1974), the corresponding combined standard uncertainty is 21 % for the flux. For Flux calculations the systematic error, or bias, is a big issue. The near-surface temperature gradient and skin temperatures will have an impact on the fCO_{2w} and K_0. The magnitude, along with its applicability to the bulk flux formulation under debate (McGillis and Wanninkhof, 2006; Woolf et al., 2016). For the mapped product the OISST is used. The OISST uses a variety of temperature data, including remote sensing of the skin temperature and the product is adjusted to buoy temperatures nominally at 1-m (Reynolds et al., 2007) such that implicitly a common reference depth is used for fCO_{2wMLR}. As shown in Wanninkhof et al. (2019b) the OISST was on average 0.25 ˚C lower than SST, and using the SST instead of the OISST would change the flux from -0.87 to -0.63 mol m^{-2} yr^{-1} a 27 % decrease. If OISST is used for bulk temperature and using a canonical value for difference in bulk and skin temperature of 0.17 ˚C, it would increase the uptake of CO_2 by 18 % from -0.87 to -1.04 mol m^{-2} yr^{-1} or 18 %. Based on current knowledge, we believe that using the OISST and the resulting calculated fCO_{2wMLR} as was done here yields the appropriate fluxes.

Table 2. Estimated uncertainties in measured, gridded, and mapped variables

Parameter	Method[1]	Combined Standard Uncertainty	Systematic Uncertainty[2]
fCO_{2w}	Measured	2 µatm	
SSS	Measured	0.1 per mil	
SST	Measured	0.02 ˚C	

Formatted: Font: (Default) Times New Roman, Font color: Auto
Formatted: Font: Not Bold
Formatted: Subscript
Formatted: Not Superscript/ Subscript
Formatted: Font: (Default) +Body (Times New Roman), Font color: Black
Formatted: Subscript
Formatted: Subscript
Formatted: Subscript
Formatted: Subscript
Formatted: Subscript
Formatted: Not Superscript/ Subscript
Formatted: Subscript
Formatted: Subscript
Formatted: Superscript
Formatted: Superscript
Formatted: Subscript
Formatted: Subscript
Formatted: Superscript
Formatted: Left, Line spacing: single
Formatted: Superscript
Formatted: Subscript

fCO_{2w}	Gridded	3.4 µatm	
SSS	Gridded	0.10 per mil	
SST	Gridded	0.22 ˚C	
TA	Gridded/Calculated	8 µmol kg^{-1}	
pH_T	Gridded/Calculated	0.0075	
Ω_{Ar}	Gridded/Calculated	0.2	
fCO_{2wMLR}	Mapped/MLR	6.4 µatm	Gridded fCO_{2w}-fCO_{2wMLR}= 1.5 µatm
SSS_{Hycom}	Model	0.2	Gridded SSS-SSS_{Hycom}= -0.1
OISST	Interpolated/remote sensing	0.2 ˚C	Gridded SST- OISST= 0.24˚C
TA	Mapped/Calculated	8 µmol kg^{-1}	TA_{SSS}-$TA_{SSSHycom}$=-5.25 µmol kg^{-1}
pH_T	Mapped/Calculated	.009	$pH(TA,fCO_{2w})$ – pH_T(MLR)= 0.002
Ω_{Ar}	Mapped/Calculated	0.21	0.004
Flux CO_2	Mapped/Calculated	0.18 mol m^{-2} yr^{-1}	$Flux_{SST}$- Flux OISST =0.24 mol m^{-2} yr^{-1}

1. Method refers to either the individual data point (measured); the girded value averaged on a 1˚ by1˚ by mo (gridded); or the interpolated products (mapped)
2. The systematic uncertainty is based on the difference between the different methods and products a indicated.

Note, the combined standard uncertainties and systematic uncertainties are based on average conditions

4 Datasets and data products

Several different data products are provided in conjunction with this paper. The methodology to create the products is described above, and here the file format and column headers is presented with a brief description when warranted.

4.1 Underway pCO_2 data

The quality controlled cruise data are posted at different locations. The individual cruise files with metadata can be found at https://www.aoml.noaa.gov/ocd/ocdweb/occ.html. Data can be found as part of the SOCAT holdings (Bakker et al. 2016) using an interactive graphical user interface https://ferret.pmel.noaa.gov/socat/las/. In addition, cruise files of the three ships are provided in annual directories at the National Center for Environmental Information (NCEI) (https://www.nodc.noaa.gov/ocads/oceans/VOS_Program/explorer.html). The data file structures are from the MATLAB data reduction program of Pierrot (pers. comm.).The primary identifier for the cruises is the EXPO code which is the International Council for the Exploration of the Sea (ICES) ship code and the day the ship starts the cruise. Examples are as follows: For a cruise of the *EoS* starting March 6, 2002, the EXPO code is 33KF20020330; for a *ALos* cruise starting

Formatted: Superscript
Formatted: Subscript
Formatted: Left, Line spacing: single
Formatted: Subscript
Formatted: Subscript
Formatted: Left, Line spacing: single
Formatted: Subscript
Formatted: Left, Line spacing: single
Formatted: Left, Line spacing: single
Formatted: Subscript
Formatted: Subscript
Formatted: Subscript
Formatted: Left, Line spacing: single
Formatted: Subscript
Formatted: Not Superscript/ Subscript
Formatted: Left, Line spacing: single
Formatted: Subscript
Formatted: Superscript
Formatted: Superscript
Formatted: Left, Line spacing: single
Formatted: Subscript
Formatted: List Paragraph, Numbered + Level: 1 + Numbering Style: 1, 2, 3, … + Start at: 1 + Alignment: Left + Aligned at: 0.25" + Indent at: 0.5"
Deleted: is
Moved down [6]: The data file structure is from the MATLAB data reduction program of Pierrot (pers. comm.). The individual
Deleted: in annual folders
Deleted:
Moved (insertion) [6]
Deleted: is
Deleted: *AoS*

November 25, 2018, the EXPO code is BHAF20181125, and for the *Eqnx* cruise departing her homeport on February 10, 2018, it is MLCE20180210. The individual cruise files at the sites above sometimes include data outside the study region.

4.2 Gridded data

The gridded datasets are the binned and averaged fCO_{2w}, SST, and SSS observations on a (1˚ by 1˚ by mo) grid. The files include the auxiliary data obtained from remote sensing and interpolated data (OISST), data assimilation of remotely sensed winds (CCMP-2) ,and from the HYCOM model (SSS_{HYCOM}). Calculated TA, pH_T and Ω_{Ar} using procedures outlined above are provided in the file. The calculated fCO_{2w} using the annual MLRs (Table 1) are provided as well. This gridded data set has spatial and temporal gaps as the ships did not transit through each pixel, and coverage is uneven. The number of observations differ for each grid cell and are listed in the gridded data set. For the auxiliary data the number of data points are fixed by the resolution of the data products except where part of the grid includes land which is masked. The column headers are provided in Table 3 and include units and descriptions when warranted.

Table 3. Column headers for the monthly 1-degree gridded observational product (1˚ by 1˚ by mo)

Parameter	Unit	Description
Year		
Month		1 (January) through 12 (December)
Latitude (Lat)	Degrees	North is positive. Location is the center point of the grid cell. That is, 15.5˚ N is the grid box spanning 15˚ N to 16˚ N
Longitude (Lon)	Degrees	East is positive. All values in the Caribbean are negative. Location is center point of the grid cell. That is, -87.5 is the grid box spanning 87˚ W to 88˚ W
Area	Km^2	Area of grid box excluding land where appropriate
#_Obs		Number of fCO_{2w} observations in the particular grid box for the particular month
SST_OBS	˚C	Sea surface temperature measured at the intake (average of the grid box)
SST_STDEV	˚C	Standard deviation of SST
SSS_OBS	permil	Sea surface salinity measured by thermosalinograph (average of the grid box)
SSS_STDEV	permil	Standard deviation of SSS
fCO_{2w}_OBS	µatm	Fugacity of CO_2 in seawater (average of the grid box)
fCO_{2w}_STDEV		Standard deviation of fCO_{2w} observations in the grid box
TA	µmol kg^{-1}	Total alkalinity calculated from a relationship salinity TA = 57.3SSS_OBS+ 296.4 (Cai et al., 2010) using the measured SSS
pH_T		pH on the total scale at SST calculated from fCO_{2w}_OBS and TA using the CO2SYS program of Pierrot et al. (2006) with pH Scale: Total scale (mol/kg-SW)

Deleted: point
Deleted: included
Deleted: 2
Deleted: ¶
Deleted: 2
Deleted: Lat
Deleted:
Deleted: Lon

		at OISST; CO_2 Constants: K1, K2 from Lueker et al. (2000); KSO_4^- for Dickson (1990); KF from Perez and Fraga (1987) and Total Boron from Uppström (1974)
Ω_{Ar}		Aragonite saturation state calculated using CO2SYS with fCO_{2w}_OBS and TA as input parameters and the same dissociation constants as used for pH_T
OISST	˚C	Optimal interpolated sea surface temperature (Reynolds et al., 2007) for the particular grid box
SSS_{HYCOM}	permil	Sea surface salinity from the HYCOM model
fCO_{2w_MLR}	µatm	Fugacity of CO_2 in seawater determined from annual MLRs (see Table 1) with Lat, Lon, SST, OISST, SSS_{HYCOM}, and MLD_{HYCOM}.

Deleted: _

Formatted: Subscript

4.3 Mapped product

The mapped product provides the data on a homogeneous (1° by 1° by mo) grid boxes utilizing the annual MLRs of fCO_{2w} as a function of Lat, Lon, OISST, SSS_{HYCOM}, and MLD_{HYCOM} for the region from 15° N to 28° N and -62° to -88° (= 62° W to 88° W). The modeled and remotely sensed products OISST, SSS_{HYCOM}, and MLD_{HYCOM}, and position were used in the MLR (Eq. 4) as the independent parameters. The mapped product includes the air-sea CO_2 fluxes in the region as a specific flux (mol m^{-2} yr^{-1}) for each grid box. The column headers are provided in Table 4 including units and descriptions when warranted.

Table 4. Column headers for the monthly 1-degree mapped product (1° by 1° by mo) for the whole region

Parameter	Unit	Description
Year		
Month		1 (January) through 12 (December)
Latitude (Lat)	Degrees	North is positive. Location is center point of the grid cell. For example, 15.5° N is the grid box spanning 15° N to 16° N
Longitude (Lon)	Degrees	East is positive. All values in Caribbean are negative. Location is center point of the grid cell. For example, -87.5 is the grid box spanning 87° W to 88° W
Area	Km^2	Area of grid box excluding land where appropriate
OISST	°C	Optimal interpolated sea surface temperature (Reynolds et al., 2007)
SSS_{HYCOM}	permil	Sea surface salinity Sea surface salinity from HYCOM
MLD_{HYCOM}	m	Mixed layer depth from the HYCOM model
fCO_{2wMLR}	µatm	Fugacity of CO_2 in seawater determined from annual MLRs with Lat, Lon, SST, SSS, and MLD (see Table 1)
fCO_{2a}	µatm	Fugacity of CO_2 in air using the average value between atmospheric sampling station KEY and RBP
ΔfCO_2	µatm	Air water fugacity difference, fCO_{2w} - fCO_{2a}
TA	µmol kg^{-1}	Total alkalinity calculated from a relationship salinity TA = $57.3SSS_{HYCOM}$+ 296.4 (Cai et al., 2010)
pH_T		pH calculated from fCO_{2w} and TA with the CO2SYS program of Pierrot et al. (2006) with pH Scale: Total scale (mol/kg-SW) at OISST; CO_2 Constants: K1, K2 from Lueker et al. (2000); KSO_4^- for Dickson (1990); KF from Perez and Fraga (1987) and Total Boron from Uppström (1974)
Ω_{Ar}		Aragonite saturation state calculated using CO2SYS with fCO_{2wMLR}, TA, OISST,

Deleted: The comparison between observed SST and OISST showed that the OISST was on average 0.25 ˚C lower than SST. The SSS_{HYCOM} was 0.10 higher than SSS. The average difference between fCO_{2w}_OBS and fCO_{2wMLR} was 1.5 µatm with the fCO_{2w_OBS} being higher. While the differences are within the standard deviation, they are possibly real due to known near-surface gradients in the region. No attempt was made to normalize the SST and SSS to OISST and SSS_{HYCOM}. ¶ ¶

Deleted: data

Deleted: data

Deleted: extends

Deleted: observations

Deleted: through gap filling of missing

Deleted:

Moved (insertion) [5]

Deleted: .

Deleted: :

Moved up [5]: OISST, SSS_{HYCOM}, and MLD_{HYCOM}.

Deleted: As noted above, the ΔfCO_2 using OISST compared to SST_OBS was 1.5 µatm smaller leading to a larger average CO_2 flux into the ocean. Wanninkhof et al. (2019b) showed a 27 % decrease in average specific uptake of CO_2 from -0.87 to -0.63 mol m^{-2} yr^{-1} if SST rather than OISST was used for the 2002-2017 time period. …

Deleted: 3

Deleted: 3

Formatted: Not Superscript/ Subscript

		and SSS_{HYCOM} as input parameters with same dissociation constants as used for pH_T
$<u^2>$	$m^2\ s^{-2}$	Second moment of the wind based on ¼° 6-h CCMP-2 product (Atlas et al., 2011)
CO_2_Flux	mol $m^{-2}\ yr^{-1}$	Monthly air-sea CO_2 flux calculated according to Eqs. 5 and 6, with fCO_{2wMLR} @ OISST

430

4.4 Monthly and Annual estimates for the Caribbean 2002-2018

Summary files of monthly and annual data and products covering the whole region from 15º N to 28° N and 88º W and 62° W are provided based on averaging or summing the data in the mapped products. The column headers for the monthly and annual products are similar (Tables 5 and 6). For the monthly files the average of each parameter for each cell are area
435 weighted based on the area of the cell as provided in the mapped product (Table 4) according to: area cell/(total area/#of cells). The total CO_2 mass flux (CO_2 $Flux_{Total}$) is the integral of the monthly area weighted CO_2 fluxes (mol $m^{-2}\ yr^{-1}$) expressed in teragrams carbon (= 10^{12} g C) per month or per year.

Table 5. Column headers for the monthly averaged mapped product

Parameter	Unit	Description
Year		
Month		1 (January) through 12 (December)
Area	km^2	Total area of Caribbean region excluding land (15° N to 28° N and 62° W to 88° W)
OISST	°C	Optimal interpolated sea surface temperature (Reynolds et al., 2007)
SSS_{HYCOM}	permil	Sea surface salinity Sea surface salinity from HYCOM
MLD_{HYCOM}	m	Mixed layer depth from the HYCOM model
fCO_{2wMLR}	µatm	Fugacity of CO_2 in seawater determined from annual MLRs with Lat, Lon, SST, SSS, and MLD (see Table 1)
fCO_{2a}	µatm	Fugacity of CO_2 in air using the average value between atmospheric sampling station KEY and RBP
ΔfCO_2	µatm	Air-water fugacity difference, fCO_{2w} - fCO_{2a}
TA	µmol kg^{-1}	Total alkalinity calculated from a relationship salinity TA = $57.3SSS_{HYCOM}$+ 296.4 (Cai et al., 2010)
pH_T		pH calculated from fCO_{2w} and TA with the CO2SYS program of Pierrot et al. (2006) with pH Scale: Total scale at OISST; CO_2 Constants: K1, K2 from Lueker

Deleted: n
Deleted: 4
Deleted: 5
Formatted: Subscript
Deleted: 5
Deleted: , and provided in
Deleted:
Deleted: 4
Deleted: 5
Deleted:
Deleted: The standard deviations of the monthly files represent the spatial deviations of the sums and averages for the monthly grid boxes for the region. For the annual files, the standard deviation (stdev) is the temporal deviation based on the monthly averages (n=12). The averages were weighted according to area of each 1° by
Deleted: The averages were weighted according to area of each 1° by 1°grid box. …
Deleted: -
Deleted: ¶
Of note is that the quantities, such as TA, pH_T, Ω_A, and CO_2-Flux, are not calculated from the variables presented as monthly or annual parameters but rather they are sums of the monthly grid boxes. For example, the monthly average TA is the area weighted average of the TA calculated for each grid box which will not be the same as using the parameterization, TA=$57.3SSS_{HYCOM}$+ 296.4 and the monthly averaged SSS_{HYCOM}.¶
Deleted: 4
Deleted: (mol/kg-SW)

		et al. (2000); KSO_4^- for Dickson (1990); KF from Perez and Fraga (1987) and Total Boron from Uppström (1974)
Ω_{Ar}		Aragonite saturation state calculated using CO2SYS with fCO_{2wMLR}, TA, OISST, and SSS_{HYCOM} as input parameters with same dissociation constants as used for pH_T
$<u^2>$	$m^2\ s^{-2}$	Second moment of the wind based on ¼˚ 6-h CCMP-2 product (Atlas et al., 2011)
CO_2_Flux	mol m^{-2} mo^{-1}	Monthly air-sea CO_2 flux calculated according to Eqs. 5 and 6
CO_2_$Flux_{Total}$	Tg C mo^{-1}	Total monthly air-sea CO_2 flux calculated according to Eqs. 5 and 6 in Teragram carbon

Table 6. Column headers for the annual averaged mapped product

Year		
Area	km^2	Total area of Caribbean region, excluding land, from 15˚ N to 28˚ N and 62˚ W to 88˚ W
OISST	˚C	Optimal interpolated sea surface temperature (Reynolds et al., 2007)
SSS_{HYCOM}	permil	Sea surface salinity Sea surface salinity from HYCOM
MLD_{HYCOM}	m	Mixed layer depth from the HYCOM model
Area	Km^2	Area of grid box excluding the surface area of land where appropriate
fCO_{2wMLR}	µatm	Fugacity of CO_2 in seawater determined from annual MLRs with Lat, Lon, SST, SSS, and MLD (see Table 1)
fCO_{2a}	µatm	Fugacity of CO_2 in air using the average value between atmospheric sampling station KEY and RBP
ΔfCO_2	µatm	Air water fugacity difference, fCO_{2w} - fCO_{2a}
TA	µmol kg^{-1}	Total alkalinity calculated from a relationship salinity TA = $57.3SSS_{HYCOM}$+ 296.4 (Cai et al., 2010)
pH_T		pH calculated from fCO_{2w} and TA with the CO2SYS program of Pierrot et al. (2006) with pH Scale: Total scale at OISST; CO_2 Constants: K1, K2 from Lueker et al. (2000); KSO_4^- for Dickson (1990); KF from Perez and Fraga (1987) and Total Boron from Uppström (1974)
Ω_{Ar}		Aragonite saturation state calculated using CO2SYS with fCO_{2wMLR}, TA, OISST, and SSS_{HYCOM} as input parameters with same dissociation constants as used for pH_T
$<u^2>$	$m^2\ s^{-2}$	Second moment of the wind based on ¼˚ 6-h CCMP-2 product (Atlas et al., 2011)

Deleted: n
Deleted: 4
Deleted: 5
Deleted: n
Deleted: 4
Deleted: 5
Deleted: -
Deleted: 5
Deleted: (mol/kg-SW)

CO_2_Flux	mol m^{-2} yr^{-1}	Annual air-sea CO_2 flux calculated according to Eqs. 5 and 6
CO_2_$Flux_{Total}$	Tg C y^{-1}	Total annual air-sea CO_2 flux calculated according to Eqs. 5 and 6 in Teragram carbon

Deleted: n
Deleted: 4
Deleted: 5
Deleted: n
Deleted: 4
Deleted: 5
Deleted: -

5 Data availability

The observations are available at three locations in slightly different formats but all files are stored by ship and cruise. The primary source is the website at the Atlantic Oceanographic and Meteorological Laboratory (AOML) (https://www.aoml.noaa.gov/ocd/ocdweb/occ.html). These data are submitted to SOCAT at least once a year such that they can be posted in the annual updates of SOCAT (https://socat.info). The permanent depository of the data is at NCEI where the data are stored per cruise in directories listed per year (https://www.nodc.noaa.gov/ocads/oceans/VOS_Program/explorer.html). The gridded observations and mapped products described herein are posted at directories at AOML and NCEI. The dataset, and derived quantities are provided on a 1-degree monthly grid at http://accession.nodc.noaa.gov/0207749, DOI:10.25921/2swk-9w56 (Wanninkhof et al., 2019a). The products cover the years 2002 through 2018 and will be updated annually.

6 Conclusions

The datasets from the cruise ships sailing the Caribbean Sea are a rich resource for studying the trends and patterns of inorganic carbon cycling and ocean acidification in the region. The scales of variability and data density are such that the (1° by 1° by mo) monthly gridding captures the magnitudes and trends of fCO_{2w} and derived inorganic carbon products on seasonal to interannual scales. Using annual MLRs to interpolate fCO_{2w} with position, SST, SSS, and MLD as independent variables yielded accurate monthly products (Wanninkhof et al., 2019a). A comprehensive investigation of the changes in decadal trends based on the dataset and products was presented in Wanninkhof et al. (2019b). The combined standard uncertainties and systematic offsets of gridding and mapping were estimated from comparing fCO_{2w} observations with gridded and mapped products including TA, pH_T and Ω_A. The MLRs capture the spatial and temporal variability in fCO_{2w} and calculated pH_T and Ω_{Ar} well in the region. The datasets and products are invaluable for model initiation and validation, and serve as boundary conditions for near-shore fine scale models.

Deleted: is
Deleted: degree
Deleted: binning
Deleted:
Deleted:
Deleted: ,
Deleted: and
Deleted: are used to determine the artifacts and biases that can occur from extrapolation of data.

Team list

This work was done on Royal Caribbean Cruise Lines (RCCL) ships who provided access, and personnel and infrastructure resources for the measurement campaign coordinated through the Rosenstiel School of Marine and Atmospheric Sciences

Deleted: would not have been possible without support from
Deleted:
Deleted: have
Deleted:
Deleted: to their ships and significant financial,

(RSMAS) of the University of Miami (U. Miami). Peter Ortner, Elizabeth Williams, Don Cucchiara and Chip Maxwell of the Marine Technical group at RSMAS/U. Miami have been instrumental in maintaining the science operations. Denis Pierrot, Kevin Sullivan, Leticia Barbero, Robert Castle (ret.), and Betty Huss of NOAA/AOML have led the gathering, maintenance, data processing and posting of fCO_2 data. In addition to fCO_2 measurements; skin temperature (MAERI), led by P. Minnet and M. Izaguirre, RSMAS; TSG with instruments, supplied by G. Goni and F. Bringas of AOML; optics, and ADCP, with data processed at the University of Hawaii Currents center (E. Firing and J. Hummon), operations take place on the RCCL ships.

Deleted: keeping the science operations going

Deleted: NOAA

Deleted: ,

Author contributions

All authors contributed to writing and editing the documents. JT performed most of the gridding and binning, and provided the model and remotely sensed data from the sources listed in the text. KF and DP performed maintenance and data reduction, and liaised with all parties involved in the operations.

Competing interests

The authors of this manuscript have no competing interest involving this work.

Acknowledgments

This work would not have been possible without support from Royal Caribbean Cruise Lines who have provided access to their ships and significant financial, personnel, and infrastructure resources for the measurement campaign coordinated through the Rosenstiel School of Marine and Atmospheric Sciences of the University of Miami. David Munro INSTAR, ESRL/GMD provided the KEY and RPB CO_2 data. NOAA Optimal Interpolated SST data were provided by the NOAA/OAR/ESRL PSD. The NOAA office of Oceanic and Atmospheric Research (OAR) is acknowledged for financial support, in particular the Ocean Observations and Monitoring Division (OOMD) (fund reference 100007298), and the NOAA/OAR Ocean Acidification Program.

Deleted:

Deleted: through

Deleted: https://www.esrl.noaa.gov/psd/

Deleted: oceanic

Deleted: atmospheric

Deleted: research

References

Atlas, R., Hoffman, R. N., Ardizzone, J., Leidner, S. M., Jusem, J. C., Smith, D. K., and Gombos, D.: A cross-calibrated multiplatform ocean surface wind velocity product for meteorological and oceanographic applications, Bull. Amer. Meteor. Soc., 92, 157-174, doi: 10.1175/2010BAMA2946.1, 2011.

Bakker, D. C. E., Pfeil, B., Landa, C. S., Metzl, N., O'Brien, K. M., Olsen, A., Smith, K., Cosca, C., Harasawa, S., Jones, S. D., Nakaoka, S. I., Nojiri, Y., Schuster, U., Steinhoff, T., Sweeney, C., Takahashi, T., Tilbrook, B., Wada, C., Wanninkhof, R., Alin, S. R., Balestrini, C. F., Barbero, L., Bates, N. R., Bianchi, A. A., Bonou, F., Boutin, J., Bozec, Y., Burger, E. F., Cai, W. J., Castle, R. D., Chen, L., Chierici, M., Currie, K., Evans, W., Featherstone, C., Feely, R. A., Fransson, A., Goyet, C., Greenwood, N., Gregor, L., Hankin, S., Hardman-Mountford, N. J., Harlay, J., Hauck, J., Hoppema, M., Humphreys, M. P., Hunt, C. W., Huss, B., Ibánhez, J. S. P., Johannessen, T., Keeling, R., Kitidis, V., Körtzinger, A., Kozyr, A., Krasakopoulou, E., Kuwata, A., Landschützer, P., Lauvset, S. K., Lefèvre, N., Lo Monaco, C., Manke, A., Mathis, J. T., Merlivat, L., Millero, F. J., Monteiro, P. M. S., Munro, D. R., Murata, A., Newberger, T., Omar, A. M., Ono, T., Paterson, K., Pearce, D., Pierrot, D., Robbins, L. L., Saito, S., Salisbury, J., Schlitzer, R., Schneider, B., Schweitzer, R., Sieger, R., Skjelvan, I., Sullivan, K. F., Sutherland, S. C., Sutton, A. J., Tadokoro, K., Telszewski, M., Tuma, M., Van Heuven, S. M. A. C., Vandemark, D., Ward, B., Watson, A. J., and Xu, S.: A multi-decade record of high-quality fCO_2 data in version 3 of the Surface Ocean CO2 Atlas (SOCAT), Earth Syst. Sci. Data 8, 383-413, doi:10.5194/essd-8-383-2016, 2016.

Boutin, J., Merlivat, L., Henocq, C., Martin, N., and Sallee, J. B.: Air–sea CO_2 flux variability in frontal regions of the Southern Ocean from CARbon Interface OCean Atmosphere drifters, Limnol and Oceanogr., 53, 2062-2079, 2008.

Cai, W.-J., Hu, X., Huang, W.-J., Wang, Y., Peng, T.-H., and Zhang, X.: Alkalinity distribution in the Western North Atlantic Ocean margins, J Geophys. Res., 115, doi:10.1029/2009JC005482, 2010.

Copernicus Climate Change Service (C3S) (2017): ERA5: Fifth generation of ECMWF atmospheric reanalyses of the global climate. Copernicus Climate Change Service Climate Data Store (CDS), *date of access July 9, 2019*. https://cds.climate.copernicus.eu/cdsapp#!/home

CarbonTracker Team Compilation of near real time atmospheric carbon dioxide data; obspack_co2_1_NRT_v4.4.2_2019-06-10; NOAA Earth System Research Laboratory, Global Monitoring Division. http://doi.org/10.25925/20190610, 2019.

DeGrandpre, M. D., Olbu, G. J., Beatty, C. M., and Hammar, T. R.: Air–sea CO_2 fluxes on the US Middle Atlantic Bight, Deep Sea Research Part II: Topical Studies in Oceanography, 49, 4355-4367, 2002.

Dickson, A. G.: Standard potential of the reaction: AgCl(s) + 1/2 H_2(g) = Ag(s) + HCl(aq), and the standard acidity constant of the ion HSO_4^- in synthetic seawater from 273.15 to 318.15 K, Journal of Chemical Thermodynamics 22, 113-127, 1990.

Evans, W., Mathis, J. T., Cross, J. N., Bates, N. R., Frey, K. E., Else, B. G. T., Papkyriakou, T. N., DeGrandpre, M. D., Islam, F., Cai, W.-J., Chen, B., Yamamoto-Kawai, M., Carmack, E., Williams, W. J., and Takahashi, T.: Sea-air CO_2

exchange in the western Arctic coastal ocean, Global Biogeochemical Cycles, 2015GB005153, 10.1002/2015gb005153, 2015.

Gledhill, D. K., Wanninkhof, R., Millero, F. J., and Eakin, M.: Ocean acidification of the greater Caribbean region 1996-2006, J Geophys. Res., 113, C10031, doi:10.1029/2007JC004629, 2008.

Gomez, F. A., Wanninkhof, R., Barbero, L., Lee, S. K., and Hernandez Jr, F. J.: Seasonal patterns of surface inorganic carbon system variables in the Gulf of Mexico inferred from a regional high-resolution ocean biogeochemical model, Biogeosciences, 17, 1685-1700, 10.5194/bg-17-1685-2020, 2020.

Jiang, L.-Q., R. A. Feely, B. R. Carter,, D. J. Greeley, D. K. G., and, and Arzayus, K. M.: Climatological distribution of aragonite saturation state in the global oceans, Global Biogeochem Cycles, 29, doi:10.1002/2015GB005198, 2015.

Lauvset, S. K., Key, R. M., Olsen, A., Heuven, S. v., A. Velo, Lin, X., C. Schirnick, Kozyr, A., T. Tanhua, Hoppema, M., Jutterström, S., R. Steinfeldt, Jeansson, E., Ishii, M., Pérez, F. F., Suzuki, T., and Watelet:, S.: A new global interior ocean mapped climatology: the 1°x1° GLODAP version 2, Earth Syst. Sci. Data, 8, 325–340, doi:10.5194/essd-8-325-2016, 2016.

Lee, K., Tong, L. T., Millero, F. J., Sabine, C. L., Dickson, A. G., Goyet, C., Park, G.-H., Wanninkhof, R., Feely, R. A., and Key, R. M.: Global relationships of total alkalinity with salinity and temperature in surface waters of the world's oceans Geophys. Res. Let., 33, L19605, doi:19610.11029/12006GL027207, 022006, 2006.

Lueker, T. J., Dickson, A. G., and Keeling, C. D.: Ocean pCO_2 calculated from dissolved inorganic carbon, alkalinity, and equations for K1 and K2; validation based on laboratory measurements of CO_2 in gas and seawater at equilibrium, Mar. Chem., 70, 105-119, 2000.

McGillis, W., and Wanninkhof, R.: Aqueous CO2 gradients for air-sea flux estimates, Marine Chemistry, 98, 100-108, 2006.

Millero, F. J., Lee, K., and Roche, M.: Distribution of alkalinity in the surface waters of the major oceans, Mar. Chem., 60, 111-130, 1998.

Minnett, P. J., Knuteson, R. O., Best, F. A., Osborne, B. J., Hanafin, J. A., and Brown, O. B.: The Marine-Atmospheric Emitted Radiance Interferometer: A high-accuracy, seagoing infrared spectroradiometer, Journal of Atmospheric and Oceanic Technology, 18, 994-1013, doi:10.1175/1520-0426, 2001.

Deleted: Gomez, F. A., Lee, S. K., Liu, Y., Hernandez Jr, F. J., Muller-Karger, F. E., and Lamkin, J. T.: Seasonal patterns in phytoplankton biomass across the northern and deep Gulf of Mexico: a numerical model study, Biogeosciences, 15, 3561-3576, doi:10.5194/bg-15-3561-2018, 2018.¶

Deleted: ¶

Deleted: ¶
Millero, F. J.: Thermodynamics of the carbon dioxide system in the oceans, Geochimica et Cosmochimica Acta, 59, 661-677, 1995.¶

Mollica, N. R., Guo, W., Cohen, A. L., Huang, K.-F., Foster, G. L., Donald, H. K., and Solow, A. R.: Ocean acidification affects coral growth by reducing skeletal density, Proceedings of the National Academy of Sciences, 115, 1754, 10.1073/pnas.1712806115, 2018.

Mucci, A.: The solubility of calcite and aragonite in seawater at various salinities, temperatures, and one atmosphere total pressure, Am. J. of Science, 283, 780-799, 10.2475/ajs.283.7.780, 1983.

Nojiri, Y. S. N., C. Miyazaki ,F. Shimano,T. Egashira, K. Kinoshita, H. Kimoto, and A. Dickson, Ocean pCO_2 System Inter-comparison at Hasaki, Japan on Feb. 2009, personal communication 2009.

Orr, J. C., Epitalon, J.-M., Dickson, A. G., and Gattuso, J.-P.: Routine uncertainty propagation for the marine carbon dioxide system, Marine Chemistry, 207, 84-107, https://doi.org/10.1016/j.marchem.2018.10.006, 2018.

Perez, F. F., and Fraga, F.: A precise and rapid analytical procedure for alkalinity determination, Mar. Chem., 21, 169-182, 1987.

Pierrot, D., Lewis, E., and Wallace, D. W. R.: MS Excel program developed for CO2 system calculations, ORNL/CDIAC-105a. ed., Carbon Dioxide Information Analysis Center, Oak Ridge National Laboratory, U.S. Department of Energy, Oak Ridge, Tennessee. doi: 10.3334/CDIAC/otg.CO2SYS_XLS_CDIAC105a, 2006.

Pierrot, D., Neil, C., Sullivan, K., Castle, R., Wanninkhof, R., Lueger, H., Johannson, T., Olsen, A., Feely, R. A., and Cosca, C. E.: Recommendations for autonomous underway pCO_2 measuring systems and data reduction routines, Deep -Sea Res II, 56, 512-522, 2009.

Purkis, S., Cavalcante, G., Rohtla, L., Oehlert, A., Harris, P.M., and Swart, P.: Hydrodynamic control of whitings on Great Bahama Bank, Geology, 45(10), 939-942, 10.1130/G39369.1, 2017.

Reynolds, R. W., Smith, T. M., Liu, C., Chelton, D. B., Casey, K. S., and Schlax, M. G.: Daily high-resolution blended analyses for sea surface temperature, *J. Climate*, 20, 5473-5496, 2007.

Riley, J. P., and Tongudai, M.: The major cation/chlorinity ratios in sea water, Chemical Geology, 2, 263-269, https://doi.org/10.1016/0009-2541(67)90026-5, 1967.

Deleted: ¶

Deleted: ¶

Deleted: analyitical

Schuster, U., McKinley, G., Bates, N., Chevalier, F., Doney, S. C., Fay, A. R., Gonzalez-Davila, M., Gruber, N., Jones, S., Landschützer, P., Lefevre, N., Manizza, M., Mathis, J. T., Metzl, N., Olsen, A., Santana-Casiano, J. M., Takahashi, T., Wanninkhof, R., and Watson, A.: Atlantic and Artic Sea-air CO_2 fluxes, 1990-2009, Biogeosciences Discuss., 9, 10669-10724, 10.5194/bgd-9-10669-2012, 2012.

Takahashi, T., Sutherland, S. C., Chipman, D. W., Goddard, J. C., Ho, C., Newberger, T., Sweeney, C., and Munro, D. W.: Climatological distributions of pH, pCO_2, total CO_2, alkalinity, and $CaCO_3$ saturation in the global surface ocean, and temporal changes at selected locations, Mar. Chem., 164, 95-125, http://dx.doi.org/10.1016/j.marchem.2014.06.004, 2014.

Takahashi, T., Sutherland, S. C., and Kozyr, A.: Global Ocean Surface Water Partial Pressure of CO_2 Database: Measurements Performed During 1957-2017 (LDEO Database Version 2017) (NCEI Accession 0160492). Version 4.4. NOAA National Centers for Environmental Information. LDEOv2017, 2018.

Takahashi, T., Sutherland, S. C., Wanninkhof, R., Sweeney, C., Feely, R. A., Chipman, D. W., Hales, B., Friederich, G., Chavez, F., Sabine, C., Watson, A., Bakker, D. C. E., Schuster, U., Metzl, N., Inoue, H. Y., Ishii, M., Midorikawa, T., Nojiri, Y., Koertzinger, A., Steinhoff, T., Hoppema, M., Olafsson, J., Arnarson, T. S., Tilbrook, B., Johannessen, T., Olsen, A., Bellerby, R., Wong, C. S., Delille, B., Bates, N. R., and de Baar, H. J. W.: Climatological mean and decadal change in surface ocean pCO_2, and net sea-air CO_2 flux over the global oceans, Deep -Sea Res II, 2009, 554-577, doi:10.1016/j.dsr2.2008.12.009, 2009.

Uppström, L. R.: The boron/chloronity ratio of deep-sea water from the Pacific Ocean, Deep-Sea Research, 21, 161-162, 1974.

Wanninkhof, R., Pierrot, D., Sullivan, K.F., Barbero, L., Triñanes, J. A. A 17-year dataset of surface water fugacity of carbon dioxide (fCO_2), along with calculated pH, aragonite saturation state, and air-sea CO_2 fluxes in the Caribbean Sea, Gulf of Mexico and North-East Atlantic Ocean covering the timespan from 2003-03-01 to 2018-12-31, (NCEI Accession 0207749). NOAA National Centers for Environmental Information. Dataset. https://accession.nodc.noaa.gov/0207749. Accessed [date]. https://doi.org/10.25921/2swk-9w56, 2019a

Wanninkhof, R., Triñanes, J., Park, G.-H., Gledhill, D., and Olsen, A.: Large decadal changes in air-sea CO_2 fluxes in the Caribbean Sea. Journal of Geophysical Research, Oceans ,124 . https://doi.org/10.1029/2019JC015366. 2019b.

Wanninkhof, R.: Relationship between wind speed and gas exchange over the ocean revisited, Limnol and Oceanogr: Methods, 12, 351-362, doi:10.4319/lom.2014.12.351, 2014.

Deleted: u

Deleted: [indicate subset used].

Deleted: n

Wanninkhof, R., Bakker, D., Bates, N., Olsen, A., and Steinhoff, T.: Incorporation of alternative sensors in the SOCAT database and adjustments to dataset quality control flags, Carbon Dioxide Information Analysis Center, Oak Ridge National Laboratory, US Department of Energy, Oak Ridge, Tennessee, 25, doi:10.3334/CDIAC/OTG.SOCAT_ADQCF, 2013.

Webb, J. R., Maher, D. T., and Santos, I. R.: Automated, in situ measurements of dissolved CO_2, CH_4, and $\delta^{13}C$ values using cavity enhanced laser absorption spectrometry: Comparing response times of air-water equilibrators, Limnology and Oceanography: Methods, 14, 323-337, 10.1002/lom3.10092, 2016.

Weiss, R. F.: Carbon dioxide in water and seawater: the solubility of a non-ideal gas, Mar. Chem., 2, 203-215, 1974.

Weiss, R. F., and Price, B. A.: Nitrous oxide solubility in water and seawater, Mar. Chem., 8, 347-359, 1980.

Wilkinson, M. D., Dumontier, M., Aalbersberg, I. J., Appleton, G., Axton, M., Baak, A., Blomberg, N., Boiten, J.-W., da Silva Santos, L. B., Bourne, P. E., Bouwman, J., Brookes, A. J., Clark, T., Crosas, M., Dillo, I., Dumon, O., Edmunds, S., Evelo, C. T., Finkers, R., Gonzalez-Beltran, A., Gray, A. J. G., Groth, P., Goble, C., Grethe, J. S., Heringa, J., 't Hoen, P. A. C., Hooft, R., Kuhn, T., Kok, R., Kok, J., Lusher, S. J., Martone, M. E., Mons, A., Packer, A. L., Persson, B., Rocca-Serra, P., Roos, M., van Schaik, R., Sansone, S.-A., Schultes, E., Sengstag, T., Slater, T., Strawn, G., Swertz, M. A., Thompson, M., van der Lei, J., van Mulligen, E., Velterop, J., Waagmeester, A., Wittenburg, P., Wolstencroft, K., Zhao, J., and Mons, B.: The FAIR Guiding Principles for scientific data management and stewardship, Scientific Data, 3, 160018, doi:10.1038/sdata.2016.18, 2016.

Woolf, D. K., Land, P. E., Shutler, J. D., Goddijn-Murphy, L. M., and Donlon, C. J.: On the calculation of air-sea fluxes of CO_2 in the presence of temperature and salinity gradients, Journal of Geophysical Research: Oceans, 121, 1229-1248, 10.1002/2015JC011427, 2016.

Formatted: Subscript

Figure captions

Figure 1. Map with the cruise tracks of the *EoS*, *Eqnx*, and *ALos* from 2002 though 2018. The green rectangle depicts the region where the data and products are compared in Figure 4.

Figure 2. Histogram of number of cruises per year used in this work.

Figure 3. The difference in between fCO_{2wMLR} for subsequent months plotted versus time. The solid squares are the differences between December and January where different MLRs are used.

Figure 4. Zonal section of gridded and mapped products between 23° N and 24° N for January 2004 (Black), January 2011 (Blue), and January 2017 (Red). a. fCO_{2w}; b. SST; c. SSS. The lines with small solid circles are the mapped product, the larger solid circles are the gridded data with standard deviation of data in the box shown as error bars.

Figure 5. Relationships of surface water TA with salinity. The relationship of Cai et al. (2010), with standard error shown as error bars, is used to calculate pH and Ω_{Ar} from fCO_{2w}.

Figure 6. pH_T calculated from gridded fCO_{2w} and TA estimated from SSS, $pH_T(fCO_2,TA)$, as done in this work, minus pH_T calculated from observed fCO_{2w} and TA from SSS, $pH_T(MLR)$ plotted against temperature for the 2017 data.

Deleted: *AoS*

Deleted: 3

Deleted: 3

Deleted: and gridded data

Deleted: 4

Deleted: uncertainty

Deleted: 5

Formatted: Subscript

Formatted: Subscript

Appendix A

A 17-year dataset of surface water fugacity of CO_2, along with calculated pH, Aragonite saturation state, and air-sea CO_2 fluxes in the Caribbean Sea

Rik Wanninkhof, Denis Pierrot, Kevin Sullivan, Leticia Barbero, and Joaquin Triñanes

Multi-linear regressions (MLRs) for fCO_{2w} were applied to the data on a (1° by 1° by mo) grid using sequentially fewer independent parameters and the increase in residual was determined. This analysis was performed as two of the independent parameters used, sea surface salinity, SSS and mixed layer depth, MLD, are modeled and their accuracy is not readily known. The functional form for the multi-linear regression, MLR fit is:

$$fCO_{2w,MLR} = a\,Lon + b\,Lat + c\,SST + [d\,MLD] + [e\,SSS] + f \quad (A1)$$

Lon is longitude; Lat is latitude, and SST is sea surface temperature. The MLR with the full number of independent parameters are used in the data products described the main text and the resulting data products are in Wanninkhof et al. (2019a). The terms in brackets indicate the parameters omitted in the estimates here. The coefficients for the MLRs and their standard errors for each year without MLD, and the MLRs without MLD and SSS, are provided in Tables A1 and A2. SST and location are the strongest predictors of fCO_{2w} levels in the region. The increase in the average root mean square of the residual/error (RMSE) excluding MLD and SSS in the annual MLRs is shown in Tables A1 and A2. The average RMSE of the calculated $fCO_{2w,MLR}$ increases by 8 ± 5.5 % by excluding MLD, and increases by 11 ± 5.4 % when MLD and SSS are omitted with the annual differences provided in the last column of Tables A1 and A2.

For the entire record, from 2002-2018, single regressions of fCO_{2w} with position, SST, SSS, and MLD showed larger standard errors and coefficients of determination (r^2) as they do not capture the increase in fCO_{2w} over time due to fCO_{2w} increases in response to increasing atmospheric CO_2 levels. Regressing against ΔfCO_2 which, in principle should not have a trend over time if surface water CO_2 levels keep up with atmospheric CO_2 increases, did not improve the correlation with the independent parameters. This was attributed to the relatively small magnitude of ΔfCO_2 and the observed multi-year changes in trends of fCO_{2w} (Wanninkhof et al., 2019b). However, using the year as a variable in the regression provides a reasonable means of extrapolating over the entire time/space domain with a single regression from 3/2002 through 2/2018:

$$fCO_{2w,MLR}\ (\pm 7.8) = 23.3\ (\pm 2.0) + 1.45\ (\pm 0.02)\ (YR-2002) + 10.23\ (\pm 0.06)\ SST +$$

Deleted: x
Deleted: x
Deleted: ,
Deleted: ¶ where
Deleted: and the terms in brackets indicate the parameters omitted in the estimates here. The coefficients for the MLRs and their
Formatted: Font: Not Bold
Deleted: in Tables A1 and A2 by
Deleted: is relatively small
Deleted: estimate
Deleted: SST is the strongest predictor for the MLRs for all the years. Olsen et al. (2004) showed a strong correlation between fCO_{2w}, SST and location for the study area as well in 2003. Other observations in subtropical and tropical oceans show a similar strong correlation between fCO_{2w} and SST (e.g. Lefèvre et al. 2014; Bates et al, 2014). Including SSS and MLD improves the multi-linear regression used for spatial gap filling to some extent (Tables A1-A2). The MLD is obtained from a numerical model, as no full observational record of mixed layer depths is available for the Caribbean. The residuals of $fCO_{2w,MLR}$ versus binned fCO_{2w} for grid boxes with fCO_{2w} observations show no spatial or seasonal pattern with any of the combinations of independent variables used in Eq. A1. ¶ ¶
Deleted: uncertainty
Formatted: Superscript
Deleted: changes
Deleted: local scale variability in ΔfCO_2 that is not strongly linearly correlated with the independent variables…
Formatted: Subscript

1.19 (±0.03) Lat – 0.50 (±0.01) Lon, $r^2 = 0.84$ (A2)

where YR is the integer calendar year. Thus (YR-2002) is the year since the start of the record. The coefficient for the (YR-2002) term of 1.45 reflects the annual increase in surface water fCO_{2w} due to atmospheric fCO_{2a} increase, which averages 2.1 µatm yr^{-1} over the 2002-2018 time period.

The standard error in the $fCO_{2w,MLR}$ of 7.8 µatm in Eq. A2 is generally greater than the standard error in the annual algorithms used to fill the gaps for the annual estimates (Eq. A1) that range from 4.7 to 9.9 µatm depending on the year with an average of 6.4 µatm (Table 1 in main text).

The importance of the different independent variables for the $fCO_{2w,MLR}$ can, in part, be discerned from the standard error in the coefficients but since variables are cross-correlated, other means are investigated such as creating a MLR with either a subset or substitution of variables. Physical parameters were correlated with location (Lat, Lon) in the region. In particular, salinity showed broad correspondence with position. Therefore, substituting SSS for Lat and Lon provided similar magnitude and standard error in the coefficients of the independent variable, but a 10 % greater RMS in the estimated fCO_{2w}:

$fCO_{2w,MLR}$ (±8.8) = -238 (±9.8) +1.36 (±0.02) (YR-2002)+ 10.11 (±0.06) SST + 9.07 (±0.25) SSS, $r^2 = 0.79$ (A3)

Finally, a simple two parameter linear fit with YR and SST had reasonable predictive capability:

$fCO_{2w,MLR}$ (±9.4) = 107.2 (±1.7) +1.38 (±0.02) (YR-2002)+ 9.50 (±0.06) SST $r^2 = 0.77$ (A4)

Eq. A4 which used only SST and time showed an increase in the standard error of the derived independent variable fCO_{2w} compared to the other permutations of the MLR. This simple relationship did show some biases with location (not shown), and for gap filling to create uniform monthly fields of fCO_{2w} the full annual regressions (Table 1) using all independent parameters, SST, SSS, MLD and location was the best option.

Table A1. Coefficients for the MLR, $fCO_{2w,MLR}$ = a Lon + b Lat + c SST + e SSS + f

	a (Lon)	b (Lat)	c (SST)	f (Icept)	RMSE $fCO_{2w,MLR}$	r^2	#points	% increase RMSE**

Deleted: 46
Formatted: Subscript
Deleted: 3
Deleted: ppm
Deleted: overall uncertainty
Deleted: uncertainty
Deleted: uncertainty
Deleted: –
Deleted: uncertainty
Formatted: Tab stops: Not at 1.13" + 3.88" + 5.94"
Deleted: ¶
Deleted: →
Deleted: →
Deleted: small
Deleted: uncertainty
Deleted: gitude
Deleted: itude
Deleted: LON
Deleted: LAT

2002	-0.30	0.48	10.42	16.6	4.74	0.90	537	0.4
*	*0.04*	*0.11*	*0.17*	*25.7*				
2003	-0.53	0.35	9.60	26.7	5.32	0.86	731	2.1
	0.03	*0.09*	*0.16*	*25.1*				
2004	-0.35	0.89	11.52	-118.3	5.79	0.90	740	11.1
	0.03	*0.10*	*0.16*	*25.7*				
2005	-0.41	0.53	9.08	-198.3	6.65	0.85	664	1.1
	0.04	*0.12*	*0.15*	*31.8*				
2006	-0.20	1.26	10.23	-98.5	5.48	0.87	670	9.8
	0.03	*0.09*	*0.16*	*27.9*				
2007	-0.50	1.33	12.05	-246.0	7.96	0.74	483	13.1
	0.05	*0.17*	*0.33*	*53.0*				
2008	0.26	1.77	12.50	-138.3	6.43	0.94	107	13.6
	0.49	*0.33*	*0.32*	*65.9*				
2009	-0.38	0.24	9.26	-7.8	7.95	0.79	125	15.1
	0.25	*0.28*	*0.48*	*62.8*				
2010	-0.45	2.43	10.11	-61.4	9.66	0.84	323	3.8
	0.18	*0.26*	*0.25*	*52.6*				
2011	-0.49	1.03	8.11	-157.1	7.83	0.71	305	8.9
	0.14	*0.20*	*0.31*	*58.0*				
2012	-0.19	1.95	12.27	-253.6	8.01	0.89	358	9.9
	0.11	*0.17*	*0.24*	*54.5*				
2013	-0.13	1.89	13.04	-256.5	9.66	0.76	219	18.4
	0.21	*0.27*	*0.53*	*63.9*				
2014	-0.31	0.96	9.89	-20.1	7.40	0.76	362	5.4
	0.07	*0.15*	*0.30*	*39.5*				
2015	-0.86	0.09	7.96	23.8	6.65	0.78	455	10.6
	0.04	*0.12*	*0.30*	*37.8*				
2016	-0.75	0.32	9.57	-121.2	6.95	0.80	1001	4.4
	0.03	*0.09*	*0.18*	*16.6*				
2017	-0.42	0.56	9.49	-112	6.16	0.87	969	0
	0.03	*0.09*	*0.15*	*21.3*				

2018	-0.34	0.009	11.57	-173.2	5.35	0.89	1164	5.3
	0.02	*0.07*	*0.12*	*15.43*				

*The second row (in italics) for each annual entry is the error of the coefficient.

** The increase in root mean square error (RMSE) of $fCO_{2w,MLR}$ compared to Table 1 that includes MLD as an input

Table A2. Coefficients for the MLR, $fCO_{2w,MLR}$ = a Lon + b Lat + c SST + f

	a (Lon)	b (Lat)	c (SST)	f (Icept)	RSME $fCO_{2w,MLR}$	r^2	#points	% increase RMSE**
2002	-0.28	0.53	10.45	47.1	4.74	0.90	537	0.4
*	*0.04*	*0.10*	*0.17*	*5.3*				
2003	-0.54	0.40	9.56	60.9	5.33	0.86	731	2.3
	0.03	*0.09*	*0.16*	*5.2*				
2004	-0.37	1.14	11.30	9.4	5.89	0.90	740	13.1
	0.03	*0.09*	*0.15*	*5.0*				
2005	-0.35	1.08	8.68	84.0	7.05	0.83	664	7.1
	0.04	*0.11*	*0.16*	*5.9*				
2006	-0.18	1.56	10.06	47.8	5.59	0.86	670	12.0
	0.03	*0.07*	*0.16*	*6.4*				
2007	-0.52	1.77	11.87	-31.8	8.10	0.73	483	15.1
	0.05	*0.13*	*0.34*	*12.8*				
2008	0.46	2.17	12.42	11.9	6.50	0.93	107	14.8
	0.49	*0.30*	*0.33*	*28.4*				
2009	-0.42	0.44	9.04	82.0	7.99	0.78	125	15.6
	0.25	*0.24*	*0.46*	*20.3*				
2010	-0.45	2.67	10.11	3.8	9.67	0.84	323	3.9
	0.18	*0.18*	*0.25*	*12.4*				
2011	-0.37	1.65	7.76	101.1	8.09	0.69	305	12.5
	0.15	*0.16*	*0.31*	*14.9*				
2012	-0.18	2.42	11.95	-13.8	8.22	0.88	358	12.8
	0.12	*0.14*	*0.23*	*11.0*				
2013	-0.34	2.39	13.27	-60.7	9.88	0.75	219	21.1

Deleted: ¶
Deleted: gitude
Deleted: itude
Deleted: LON
Deleted: AT)

	0.20	*0.22*	*0.53*	*23.5*				
2014	-0.32	1.17	9.90	62.9	7.44	0.75	362	6.0
	0.07	*0.12*	*0.30*	*11.6*				
2015	-0.86	0.22	7.83	100.7	6.68	0.77	455	11.1
	0.04	*0.11*	*0.29*	*9.7*				
2016	-0.70	0.67	9.84	52.3	7.37	0.77	1001	10.7
	0.04	*0.08*	*0.19*	*6.3*				
2017	-0.40	1.07	10.33	52.8	7.02	0.83	967	13.8
	0.03	*0.08*	*0.16*	*5.32*				
2018	*-0.37*	*0.48*	*11.22*	*44.94*	5.82	0.87	1165	14.6
	0.026	*0.07*	*0.13*	*4.23*				

* The second row (in italics) for each annual entry is the error of the coefficient.

** The increase in root mean square error (RMSE) of $fCO_{2w,MLR}$ compared to Table 1 that included MLD and SSS as an independent variable.

This table is the same as Table A1 except that MLD in addition to SSS are omitted as independent variables.

References Appendix A

Wanninkhof, R., Pierrot, D., Sullivan, K.F., Barbero, L., Triñanes, J. A. A 17-year dataset of surface water fugacity of carbon dioxide (fCO_2), along with calculated pH, aragonite saturation state, and air-sea CO_2 fluxes in the Caribbean Sea, Gulf of Mexico and North-East Atlantic Ocean covering the timespan from 2003-03-01 to 2018-12-31, (NCEI Accession 0207749). NOAA National Centers for Environmental Information. Dataset. https://accession.nodc.noaa.gov/0207749. Accessed [date]. https://doi.org/10.25921/2swk-9w56, 2019a

Wanninkhof, R., Triñanes, J., Park, G.-H., Gledhill, D., and Olsen, A.: Large decadal changes in air-sea CO_2 fluxes in the Caribbean Sea. Journal of Geophysical Research, Oceans ,124 . https://doi.org/10.1029/2019JC015366. 2019b.

Formatted: Heading 1

Deleted: ¶

Bates, N. R., Astor, Y. M., Church, M. J., Currie, K., Dore, J. E., González-Dávila, M., Lorenzoni, L., Muller-Karger, F., Olafsson, J., and Santana-Casiano, J. M.: A time-series view of changing ocean chemistry due to ocean uptake of anthropogenic CO_2 and ocean acidification., Oceanography, 27, 126-141, http://dx.doi.org/10.5670/oceanog.2014.16., 2014.¶

¶

Lefèvre, N., Urbano Domingos, F., Gallois, F., and Diverrès, D.: Impact of physical processes on the seasonal distribution of the fugacity of CO_2 in the western tropical Atlantic, Journal of Geophysical Research: Oceans, 119, 646-663, 10.1002/2013JC009248, 2014.¶

¶

Olsen, A., Triñanes, J., and Wanninkhof, R.: Sea-air flux of CO_2 in the Caribbean Sea estimated using in situ and remote sensing data., Remote Sensing of Environment, 89, 309–325, 2004.…

Deleted: ¶

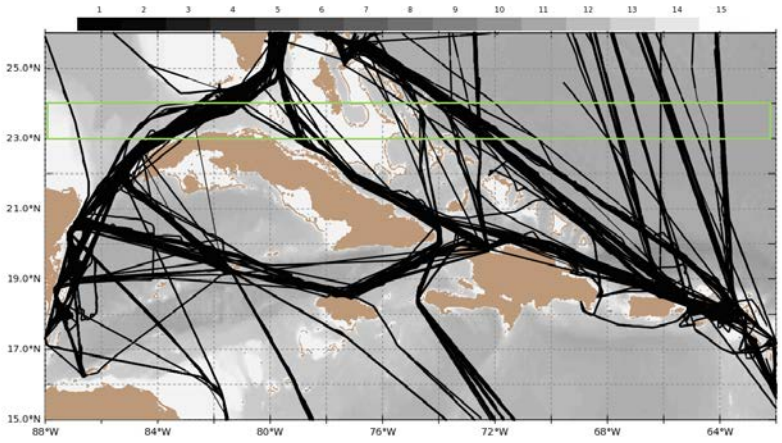
1
2
3
4
5
6
7
8
9
10
11
12
13
14
15
25.0°N
23.0°N
21.0°N
19.0°N
17.0°N
15.0°N
88°W
84°W
80°W
76°W
72°W
68°W
64°W

920

Fig 1.

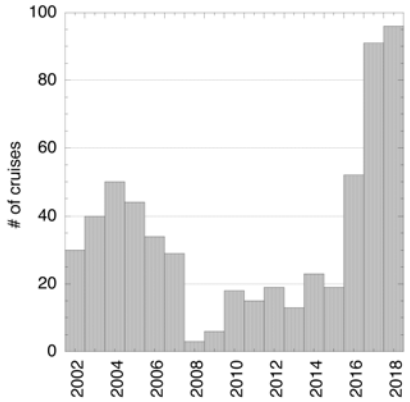
100
80
60
40
20
0
# of cruises
2002
2004
2006
2008
2010
2012
2014
2016
2018

Fig 2.

935

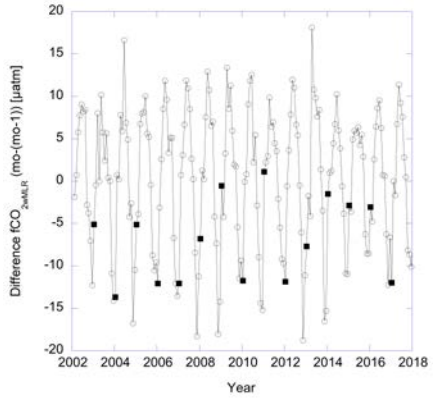
Difference fCO2wMLR (mo-(mo-1)) [µatm]
20
15
10
5
0
-5
-10
-15
-20
2002
2004
2006
2008
2010
2012
2014
2016
2018
Year

Fig. 3

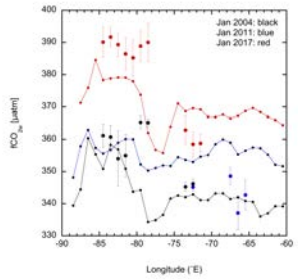

Fig. 4a

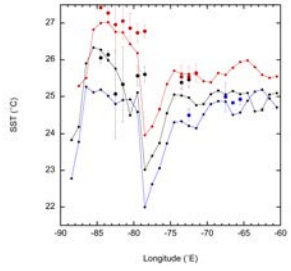

Fig. 4b

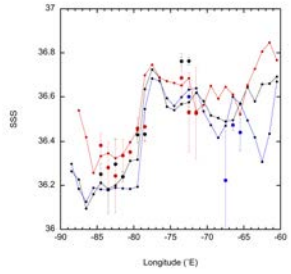

Fig. 4c

Deleted: 3a

Deleted: 3b

Deleted: 3c

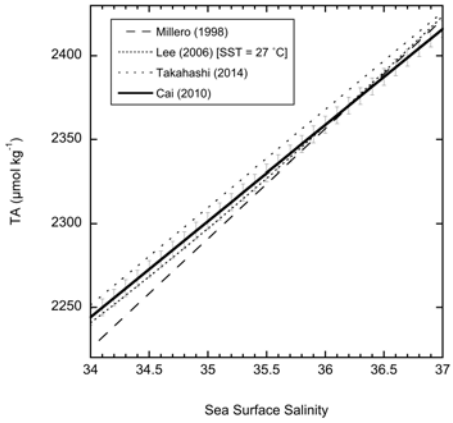

Fig. 5

Deleted: 4

950

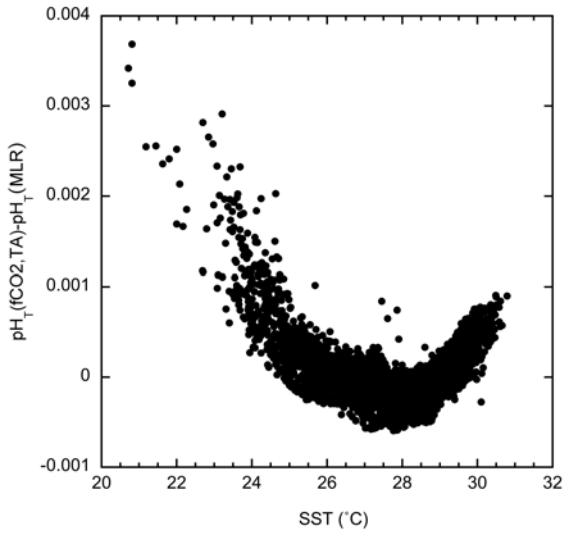

Fig. 6

Deleted: 5

1955

Page 25: [1] Deleted	Rik Wanninkhof	4/13/20 11:31:00 AM

Page 25: [1] Deleted	Rik Wanninkhof	4/13/20 11:31:00 AM

Page 25: [2] Deleted	Rik Wanninkhof	4/22/20 10:02:00 AM

Page 25: [2] Deleted	Rik Wanninkhof	4/22/20 10:02:00 AM

Page 25: [3] Deleted	Rik Wanninkhof	4/3/20 5:00:00 PM

Page 25: [3] Deleted	Rik Wanninkhof	4/3/20 5:00:00 PM

Page 25: [3] Deleted	Rik Wanninkhof	4/3/20 5:00:00 PM

Page 25: [3] Deleted	Rik Wanninkhof	4/3/20 5:00:00 PM

Page 25: [3] Deleted	Rik Wanninkhof	4/3/20 5:00:00 PM

Page 25: [3] Deleted	Rik Wanninkhof	4/3/20 5:00:00 PM

Page 25: [3] Deleted	Rik Wanninkhof	4/3/20 5:00:00 PM

Page 25: [3] Deleted	Rik Wanninkhof	4/3/20 5:00:00 PM

Page 25: [3] Deleted	Rik Wanninkhof	4/3/20 5:00:00 PM

Page 25: [4] Deleted	Rik Wanninkhof	3/26/20 11:18:00 AM

Page 25: [4] Deleted	Rik Wanninkhof	3/26/20 11:18:00 AM

Page 25: [5] Deleted	Rik Wanninkhof	4/3/20 5:23:00 PM

Page 25: [5] Deleted	Rik Wanninkhof	4/3/20 5:23:00 PM

Page 25: [5] Deleted	Rik Wanninkhof	4/3/20 5:23:00 PM

Page 25: [5] Deleted	Rik Wanninkhof	4/3/20 5:23:00 PM

Page 25: [5] Deleted	Rik Wanninkhof	4/3/20 5:23:00 PM

Page 25: [5] Deleted	Rik Wanninkhof	4/3/20 5:23:00 PM

Page 25: [5] Deleted	Rik Wanninkhof	4/3/20 5:23:00 PM

Page 25: [5] Deleted	Rik Wanninkhof	4/3/20 5:23:00 PM

Page 25: [5] Deleted	Rik Wanninkhof	4/3/20 5:23:00 PM

Page 25: [5] Deleted	Rik Wanninkhof	4/3/20 5:23:00 PM

Page 25: [5] Deleted	Rik Wanninkhof	4/3/20 5:23:00 PM

Page 25: [5] Deleted	Rik Wanninkhof	4/3/20 5:23:00 PM

Page 25: [6] Deleted	Rik Wanninkhof	4/6/20 9:50:00 AM

Page 25: [6] Deleted	Rik Wanninkhof	4/6/20 9:50:00 AM

Page 25: [6] Deleted	Rik Wanninkhof	4/6/20 9:50:00 AM

Page 25: [7] Formatted	Rik Wanninkhof	4/3/20 5:27:00 PM

Subscript

Page 25: [7] Formatted	Rik Wanninkhof	4/3/20 5:27:00 PM

Subscript

Page 25: [8] Deleted	Rik Wanninkhof	4/3/20 5:30:00 PM

Page 25: [8] Deleted	**Rik Wanninkhof**	**4/3/20 5:30:00 PM**
Page 25: [8] Deleted	**Rik Wanninkhof**	**4/3/20 5:30:00 PM**
Page 25: [8] Deleted	**Rik Wanninkhof**	**4/3/20 5:30:00 PM**
Page 25: [8] Deleted	**Rik Wanninkhof**	**4/3/20 5:30:00 PM**
Page 29: [9] Deleted	**Rik Wanninkhof**	**4/6/20 12:51:00 PM**
Page 29: [10] Deleted	**Rik Wanninkhof**	**3/26/20 3:36:00 PM**